Transportation Research Part E 205 (2026) 104520

Contents lists available at ScienceDirect

Transportation Research Part E

journal homepage: www.elsevier.com/locate/tre

Integrating geometric and causation probability approaches into Dynamic Bayesian Networks for real-time collision risk prediction

Cihad Çelik [a], Huanhuan Li [a,b,*], Jiongjiong Liu [c,d], Musa Bashir [e], Lu Zou [f,g], Zaili Yang [a,*]

[a] Liverpool Logistics, Offshore and Marine Research Institute, Liverpool John Moores University, Liverpool, UK
[b] School of Engineering, University of Southampton, Southampton, UK
[c] Intelligent Transportation System Research Center, Wuhan University of Technology, Wuhan, China
[d] National Engineering Research Center for Water Transport Safety (WTS Center), Wuhan University of Technology, Wuhan, China
[e] Department of Civil and Environmental Engineering, School of Engineering, University of Liverpool, UK
[f] School of Ocean and Civil Engineering, Shanghai Jiao Tong University, Shanghai, China
[g] State Key Laboratory of Ocean Engineering, Shanghai Jiao Tong University, Shanghai, China

ARTICLE INFO

Keywords:
Maritime transportation
Collision risk
Dynamic Bayesian Networks
AIS data
Navigational safety

ABSTRACT

Maritime transportation is vital for international trade, yet collision accidents continue to pose serious risks to navigational safety and global economic stability. This study develops a novel collision risk prediction model based on Dynamic Bayesian Networks (DBN), incorporating both geometric and causation probability approaches to realise real-time ship collision risk prediction and probabilistic risk assessment. Leveraging raw Automatic Identification System (AIS) data, the proposed model dynamically updates the probabilities of influential factors using Markov-chain-based transition analyses, mitigating uncertainties caused by noisy or incomplete data. In contrast to traditional deterministic models, the DBN captures mutual dependencies among dynamic risk factors, including variations in speed ratio, relative bearing, and temporal-spatial parameters such as Distance to Closest Point of Approach (DCPA), Time to Closest Point of Approach (TCPA) and relative distance. The model categorises collision risk into five discrete levels, ranging from very low to very high, providing decision-makers with actionable insights for real-time navigational safety. A key innovation lies in modelling these interdependencies among influential factors, which enables a holistic understanding of collision dynamics. Simulation results demonstrate that the DBN model outperforms traditional Collision Risk Index (CRI) approaches, particularly in accurately predicting complex collision scenarios and reflecting aggressive manoeuvres. This study presents a robust framework for maritime collision risk prediction, offering a foundation for enhancing navigational safety in increasingly congested and mixed-traffic environments involving the coexistence of manned and unmanned vessels.

1. Introduction

Maritime transportation is a cornerstone of global trade, enabling the movement of vast cargo volumes across international waters (Li et al., 2023a; Li et al., 2024b). Statistical analysis indicates collision is the most frequent maritime accident, and causes catastrophic

* Corresponding authors.
E-mail addresses: huanhuan.li@soton.ac.uk (H. Li), z.yang@ljmu.ac.uk (Z. Yang).

https://doi.org/10.1016/j.tre.2025.104520
Received 14 May 2025; Received in revised form 23 October 2025; Accepted 26 October 2025
Available online 7 November 2025
1366-5545/© 2025 The Author(s). Published by Elsevier Ltd. This is an open access article under the CC BY license (http://creativecommons.org/licenses/by/4.0/).

consequences when it occurs, as demonstrated by the recent accident in the North Sea (Halliday and Gayle, 2025). Although the Convention on the International Regulations for Preventing Collisions at Sea (COLREG) (IMO, 1972) provides guidance to ensure vessels take appropriate manoeuvring actions before entering critical collision zones, such regulations alone are insufficient to eliminate risk. It is therefore imperative to develop and adopt advanced technologies to continuously reduce these risks, including real-time ship collision risk prediction. However, realising real-time risk prediction for anti-collision requires effective and reliable obstacle avoidance in dynamic maritime environments, which presents a significant challenge due to the complexity of environmental conditions and vessel interactions.

Researchers have proposed various methods to improve anti-collision decision-making, which can be broadly categorised into geometrical probability and causation probability approaches (Chen et al., 2019a). The former approach is based on Euclidean calculations, while the latter calculates collision probabilities by considering influential factors such as environmental conditions, ship state, and human factors. Additionally, the geometrical probability method provides micro-scale results, such as the collision risk probability between the Own Ship (OS) and the Target Ship(s) (TS(s)), while the causation approach offers maritime stakeholders a broader perspective on the underlying causes of collision accidents.

In the geometrical probability approach, a Collision Risk Index (CRI) is frequently assessed as a synthetic indicator to represent the probability of collision risk, utilising the parameters of the Closest Point of Approach (CPA), e.g., through a collision alert system integrating CPA and expert knowledge, as introduced by Goerlandt et al. (2015). Another widely adopted method is a safe boundary approach, which establishes a spatial boundary around vessels, also known as a ship domain concept, to identify potential collision candidates. This concept was first introduced by Fujii and Tanaka (1971). Additionally, a Velocity Obstacle (VO) method determines potential collision zones by analysing the speed and heading of both the OS and TS (s) (Huang et al., 2019).

Existing collision risk assessment methods rely on a variety of parameters whose threshold values are often subjectively defined by experts and researchers. For instance, Zhang et al. (2021) defined different weight factors in CRI calculation compared to Abebe et al. (2021) and Hu et al. (2020) within the same synthetic indicator model. Similarly, while Seo et al. (2023) and Abebe et al. (2021) proposed similar collision risk levels, they adopted different threshold values in terms of CRI. Such inconsistencies introduce a degree of subjectivity and reduce the reliability of decision-making in collision risk assessment. Despite the extensive body of research on collision risk assessment, there remains a critical need for new methods and advanced technologies to improve the accuracy and effectiveness of collision candidate identification in maritime navigation.

In this study, a novel collision risk prediction model based on Dynamic Bayesian Networks (DBN) is developed to enhance real-time navigational safety. The model primarily operates within the geometric probability framework by utilising Closest Point of Approach (CPA) parameters derived from Automatic Identification System (AIS) data, but extends beyond conventional approaches by embedding causation probability principles. CPA factors are treated not merely as deterministic thresholds but as probabilistic influences within the DBN, enabling a more realistic assessment of collision risks. A key innovation lies in modelling the interdependencies among dynamic factors, including variations in speed ratio, relative bearing, relative distance, and temporal–spatial measures such as DCPA and TCPA, providing a holistic representation of evolving collision scenarios. Furthermore, the DBN employs state transition modelling to mitigate uncertainties from noisy AIS data, supporting real-time risk predictions classified into five levels: Very Low, Low, Medium, High, and Very High.

This study makes new contributions as follows:

(1) Real-time collision risk prediction.

The DBN model dynamically evaluates real-time collision risk between the OS and TS from raw AIS data, while mitigating uncertainties through the state transition mechanism of historical voyages.

(2) Integration of advanced risk factors.

Beyond traditional Euclidean-based risk measurement factors, such as DCPA, TCPA, and relative distance, the model incorporates temporal variations in speed ratio and relative bearing, enhancing prediction accuracy.

(3) Dynamic interdependency modelling.

For the first time, the model explicitly captures interdependencies among influential factors compared to prior deterministic or statistical models among dynamic influential factors, enabling a holistic and adaptive collision risk assessment.

(4) Bridging geometric and causation probability approaches.

By combining both macro-scale (causation-based) and micro-scale (geometric) perspectives, the model provides a holistic assessment of collision risks.

The structure of the paper is organised as follows: Section 2 reviews both traditional and advanced collision candidate models, alongside the applications of DBN in maritime safety, which helps to identify research gaps through a critical analysis of the existing literature. Section 3 outlines the methodological framework, beginning with an overview of the proposed approach to facilitating reader comprehension. Subsequently, a detailed procedure for dynamic collision risk assessment is presented, with particular emphasis on model verification and validation, given the innovative application of DBN in this field. Section 4 presents the practical implementation of the DBN model using real-world encounters based on AIS data and introduces a simulation scenario to evaluate its effectiveness in multi-ship encounters, particularly in prioritising collision risks among TSs. The section ends with discussions of the case study results. Section 5 provides a broader interpretation of these findings, contextualising them within COLREG and offering practical insights for maritime stakeholders. Finally, Section 6 concludes the study by summarising key findings, addressing limitations, and suggesting future research directions to enhance collision risk assessment methodologies.

2. Literature review

This section provides a critical review and identifies the corresponding research gaps. Section 2.1 explores existing collision risk models, highlighting their limitations and inherent subjectivity. Given the absence of research employing DBN for one-to-one ship encounters in collision risk assessment, the following subsection discusses the applications of DBN in maritime risk assessment only. Based on this review, the final subsection outlines the specific research gaps addressed by the paper.

2.1. Collision risk models

In a geometrical probability framework, collision risk is assessed using the CRI, which is a synthetic indicator designed to quantify the likelihood of vessel collisions. Within this framework, the CPA is widely recognised as a fundamental metric for evaluating collision scenarios. The primary factors involved in CPA-based assessments are distance and time, which are derived from AIS data, including location, bearing, and speed. These parameters are used to calculate the DCPA and TCPA, which in turn inform the calculation of the CRI through various models tailored to specific encounter configurations. The CRI is defined on a 0–1 scale, where a value of 1 denotes an immediate collision threat, whereas a value of 0 signifies no risk (Jiang et al., 2024). Beyond the synthetic indicator approach, the ship domain model, first introduced by Fujii and Tanaka (1971), offers an alternative method for collision risk evaluation. In this approach, an artificial domain is assigned around a vessel, and the degree of collision risk is determined based on the extent of interaction or overlap between these domains during navigation. Another geometric-based method is the VO approach, which predicts potential collision zones by projecting a ship's future position under the assumption that it maintains its current speed and heading. This method provides a dynamic and predictive perspective on collision risk evaluation. Table 1 presents a comparative analysis of the reviewed models, highlighting their key characteristics and distinctive features.

The COLREG establishes safe distances for manoeuvring actions in various encounter scenarios. According to these regulations, a give-way vessel should initiate manoeuvring before reaching a distance of 6 nm if the stand-on vessel is approaching from the head-on or crossing zones. In contrast, if the give-way vessel approaches the stand-on vessel from the overtaking zone, it should take action before reaching a relative distance of 3 nm. However, in complex waters and narrow channels, strict adherence to COLREG may be impractical. In such cases, manoeuvring actions can be coordinated by local authorities to ensure navigational safety. To enhance collision avoidance strategies, researchers have introduced risk-based approaches that discretise risk levels and define threshold values for steering actions based on the CRI. For example, Seo et al. (2023) categorised risk levels as low (0–0.4), medium (0.4–0.7), and high (0.7–1), recommending avoidance manoeuvres when the CRI exceeds 0.7. Similarly, Hu et al. (2020) proposed initiating steering actions at a CRI threshold of 0.6, utilising the same fuzzy inference CRI approach. Meanwhile, Abebe et al. (2021) classified risk levels into ranges of 0–0.333, 0.333–0.667, and 0.667–1, advising immediate manoeuvring action once the CRI surpasses 0.667.

A critical analysis of geometry-based collision risk assessment methods reveals that while advanced mathematical models and computational techniques have significantly improved CRI prediction, these approaches still rely to some extent on expert judgment and researcher-defined parameters, introducing an element of subjectivity and uncertainty. This reliance highlights a key limitation in current methodologies, as the accuracy of collision risk assessments may be influenced by the selection of weight factors, risk thresholds, and model parameters. To enhance the reliability and precision of collision prediction models, further research is necessary, particularly through the integration of experimental data and real-world navigational scenarios. Empirical validation of these models can help refine the existing methodologies by reducing subjectivity and improving the adaptability of risk assessment frameworks to diverse maritime environments. In addition, after a critical review of the methods summarised in Table 1, it is evident that existing studies predominantly rely on main Euclidean-based parameters to measure collision risk, particularly within the synthetic indicator approach. Yet, evidence from real collision cases shows that two additional factors, variation in speed ratio and relative bearing, also play a significant role, although they have not been incorporated into previous models. The DBN model developed in this study addresses this gap by integrating these two factors alongside the main parameters to enhance ship-to-ship collision risk prediction.

In addition to the geometric probability models, the causation-based approaches provide an alternative perspective in maritime collision risk analysis. These models assess the influence of various contributing factors by employing both traditional methods, such as Fault Tree Analysis (FTA), Functional Resonance Analysis Method (FRAM), Human Factors Analysis and Classification System (HFACS) and advanced quantitative/data-driven techniques, including BN. For instance, Ugurlu and Cicek (2022) conducted a large-scale analysis of 513 ship collision accidents spanning 45 years, applying FTA, supported by Multiple Correspondence Analysis (MCA), to examine 39 primary causal factors. From a similar perspective, Antão et al. (2023) combined Bayesian rules with the least-squares approach to analyse 936 collision events collected from the Global Integrated Shipping Information System (GISIS) database, identifying ship type and geographical area as key determinants of collision occurrence. Ma et al. (2024) employed a Frequent Pattern Growth (FP-Growth) algorithm to uncover hidden relationships among contributing factors using 285 accident reports. In another study, Shi et al. (2024) proposed a risk assessment framework for ship collisions that integrates complex network analysis with an in-house analytical approach to identify critical risk factors and support accident prevention strategies. Their analysis of 207 accident reports across 46 RIFs revealed the interdependencies among risk factors. Li et al. (2024a) performed a data-driven BN analysis using 402 accident records obtained from the GISIS and Lloyd's Register Foundation (LRF) databases. Their results identified several key RIFs that significantly contribute to collision risk, notably ship operation, information quality, and voyage segment. Besides, ship types are hierarchically ranked by risk level, with bulk carriers, tankers, and cargo ships identified as the most critical. More recently, Wang et al. (2025) advanced the causation-based analysis of collisions by enhancing FRAM with text mining. Using the most up-to-date databases, their study identified 38 risk factors, offering new insights into the complex mechanisms leading to ship collisions. It is

Table 1
Comparison of geometric probability-based models.

Approach	Method/Model	Key Characteristics	Factors Considered	References
Synthetic Indicator	Basic CRI	Utilises DCPA and TCPA with weighted factors to quantify collision risk.	DCPA, TCPA	(Jiang et al., 2024; Li et al., 2022a)
	Exponential Inference	Applies a negative exponential function where CRI increases as DCPA and TCPA decrease, with coefficients derived from expert evaluations.	DCPA, TCPA	(Ding et al., 2024; Zhen et al., 2017)
	Fuzzy Inference	Incorporates additional parameters, relative distance, bearing, and speed ratio, using fuzzy logic and expert-assigned weights to assess collision risk.	DCPA, TCPA, Relative Distance, Relative Bearing, Speed Ratio	(Hu et al., 2020)
	AHP-Based Weights in Fuzzy Inference	Employs Analytic Hierarchy Process to assign weights to factors, ensuring alignment with expert assessments; emphasises DCPA and TCPA.	DCPA, TCPA, Relative Distance, Relative Bearing, Speed Ratio	(Zhao et al., 2016)
	Fuzzy Inference	Adjusts weightings to improve reliability and reduce subjectivity in CRI assessments.	DCPA, TCPA, Relative Distance, Relative Bearing, Speed Ratio	(Jiang et al., 2024; Seo et al., 2023)
Ship Domain	Static Ship Domains	Defines a fixed area around a vessel (circular, elliptical, or polygonal) where intrusion indicates collision risk; based on the ship's dimensions and speed.	Ship Length, Breadth, Speed	(Fujii and Tanaka, 1971; Goodwin, 1975; Coldwell, 1983; Pietrzykowski and Uriasz, 2009)
	Dynamic Ship Domains	Adapts the ship domain size and shape based on dynamic factors such as speed and manoeuvrability for more accurate risk assessment.	Speed, Manoeuvrability	(Li et al., 2022c; He et al., 2024; Li et al., 2023c; Liu et al., 2023b)
	Quaternion Ship Domain (QSD)	Establishes quadrant-specific domains considering factors such as manoeuvrability, speed, and course, allowing for asymmetric domain shapes.	Course, Speed, Manoeuvrability	(Wang, 2010; Silveira et al., 2022)
	Field-Theory-Based QSD	Integrates field theory with QSD to incorporate uncertainty models for ship position prediction, enhancing collision risk identification.	Ship Dynamics, Uncertainty Models	(Qiao et al., 2021)
Velocity Obstacle	Traditional VO	Predicts potential collision zones by estimating future positions assuming constant speed and heading; typically uses a circular conflict region.	Speed, Heading	(Huang et al., 2018; Yuan et al., 2021)
	Linear/Non-Linear VO	Enhances traditional VO by incorporating linear or non-linear trajectory models to better predict collision courses.	Vessel Motion Prediction	(Huang et al., 2019; Chen et al., 2018)
	Probabilistic VO	Accounts for uncertainties in vessel movements by applying probabilistic models to predict potential collision zones.	Probabilistic Ship Paths	(Liu et al., 2024a)
	AIS-Enhanced VO	Integrates Automatic Identification System (AIS) data to dynamically model vessel behaviours, improving real-time collision risk assessment.	Real-Time Vessel Dynamics from AIS	(Zhao and Fu, 2021)
	Elliptical Conflict Region VO	Replaces the circular conflict zone with an elliptical one to more accurately represent collision risk, considering the predominant influence of a ship's fore and aft directions.	Ship Geometry (Fore/Aft Influence)	(Liu et al., 2024a)

also important to review AIS-based studies within the scope of quantitative ship collision risk. One of the earliest examples was introduced by Silveira et al. (2013), who analysed routes associated with ports along the Portuguese coast to assess collision risk using algorithms driven by AIS data. Building on this direction, Rong et al. (2021) employed spatial correlation techniques, namely Moran's I and Getis-Ord Gi*, to identify potential collision hotspots based on AIS-derived near-miss information along the Portuguese coastline. In a subsequent study, Rong et al. (2022) proposed a method to detect collision-avoidance behaviour directly from AIS trajectories, focusing specifically on evasive manoeuvres. A holistic approach, named the multi-scale collision risk estimation framework covering regional maritime traffic partition, collision risk in ship pairs and in the region, is introduced by Xin et al. (2023) to identify conflict zones in complex port waters. Researchers have also developed encounter-specific risk indicators. Liu et al. (2023b) introduced a kinematics feature-based vessel conflict ranking operator that evaluates collision risk using AIS data from vessels both at anchor and underway, successfully identifying high-risk zones within predefined areas. Similarly, Yoo and Lee (2019) proposed their own Collision Risk (CoRI) model, arguing that the Environmental Stress (ES) model, widely used in Korea's Maritime Safety Audit, fails to capture relative bearing information. Their AIS-based testing of the CoRI model covered crossing, head-on, and overtaking scenarios. Efforts have also been made to integrate AIS-based encounter data into causation probability modelling. For example, Chen et al. (2019b) developed a credal probabilistic graphical network in which micro-scale factors such as TCPA, relative bearing, and the presence of another vessel were incorporated. However, the study highlighted limitations, particularly the scarcity of accident records and challenges in linking them with historical AIS data. Extending the application of AIS beyond ship encounters, Yu et al. (2021) proposed a Bayesian-based causation risk model to evaluate ship-to-offshore platform collisions, explicitly considering ship-related and environmental conditions as the two primary causal categories. Ship conditions were defined using dependent variables such as relative distance, relative bearing, and speed, which were computed using Euclidean norms. Environmental factors, including sea state, wind, visibility, and time of day (day/night), were also integrated into the model as influential factors. The CRI was then calculated using the constructed BN model at observation points along the most frequently sailed routes, providing a dynamic assessment of collision risk.

Recent progress in intelligent maritime systems has highlighted the growing application of Artificial Intelligence (AI) and Reinforcement Learning (RL) to improve both port operations and navigational safety. Guo et al. (2025a) developed a Deep Q-network combined with domain knowledge to optimize ship operation schedules and reduce fuel use, offering an effective approach to lowering emissions and enhancing port efficiency. Furthermore, they proposed a multi-action deep reinforcement learning framework incorporating graph neural networks to jointly manage vessel scheduling and tugboat deployment, demonstrating marked gains in real-time coordination and resource utilization (Guo et al., 2025b). Liu and Yuen (2025) provided a systematic review showing that while AI adoption in seaports is expanding, its integration across different operational areas remains uneven, with reinforcement learning and neural models holding significant untapped potential. In autonomous navigation, Cui et al. (2025) introduced a Gated Transformer-based control algorithm for multi-ship collision avoidance under complex encounter conditions, whereas Pereira and Pinto (2024) designed an RL-based docking policy enabling autonomous surface vessels to manoeuvre safely in uncharted environments. These studies demonstrate how AI-driven optimization and control strategies are reshaping maritime operations and vessel autonomy, reinforcing this study's objective to embed intelligent probabilistic reasoning into collision risk prediction for autonomous navigation systems.

The literature analysis highlights two distinct yet complementary approaches to maritime collision risk assessment. The geometrical indicator approach provides a micro-scale evaluation of collision risk in ship-to-ship encounters, relying primarily on proximity-based metrics such as the CPA. While effective for real-time risk estimation, this method is limited by its dependence on predefined weight factors and risk thresholds, which may not fully capture the complexities of maritime navigation. In contrast, causation-based models offer a more comprehensive analysis by incorporating ship-specific, system-related, and environmental factors into the assessment. These models, particularly those utilising BN, enable a probabilistic evaluation of collision risk, considering the interactions between multiple influential factors. Building on these foundations, this study integrates both methodologies by identifying key RIFs through the geometrical indicator approach while interpreting their impact using a causation probability framework. By combining these techniques, our model delivers a probabilistic assessment of collision risk, providing a novel and more reliable perspective for decision-makers and autonomous navigation systems, specifically in the context of MASS. This integration enhances the robustness of collision risk assessment by reducing reliance on subjective weight assignments and improving adaptability to dynamic maritime environments.

2.2. The applications of DBN in maritime safety

DBN is a method that combines graph theory and probability theory within a temporal framework to facilitate informed decision-making. It is widely used in reliability analysis, dynamic risk assessment, and the evaluation of operational processes. This section provides a critical review of previous research on DBN, with a particular focus on its applications in maritime safety and collision risk assessment.

The safety challenges of MASS were extensively examined by Han et al. (2024), who utilised a DBN model to assess the availability of machinery systems. Their study compared traditional and autonomous systems, emphasising the importance of redundancy designs and tailored maintenance strategies to improve system reliability and reduce costs. By conducting sensitivity analyses, they offered actionable insights for the early-stage design and planning of MASS systems. Meanwhile, Yao et al. (2024) developed a fault diagnosis framework for marine diesel engines, leveraging Deep Belief Networks (DBNs) optimised with the Dragonfly Algorithm. This innovative approach addressed challenges like transient conditions and complex fault modes, significantly enhancing diagnostic accuracy and model convergence speed. In environmental risk assessment, Liu et al. (2023a) employed DBN to analyse oil spill risks during

extreme weather events. Their work integrated physical spill models with socio-economic and environmental vulnerabilities, offering dynamic insights into the spatial and temporal risks associated with oil spills under high wind conditions. Expanding on this, Zeng et al. (2024) applied DBN to model tanker oil spill scenarios caused by collisions, integrating human factors and emergency measures into a scenario-response framework. Their case study involving the MT "SANCHI" and MV "CF CRYSTAL" collision validated the practical applicability of their model. Xu et al. (2024) employed DBN to investigate the resilience of Chinese coastal ports amid disruptions caused by the COVID-19 pandemic. Their findings emphasised the critical roles of financial health and trade activity in sustaining port operations during crises. Concurrently, Fan et al. (2024b) examined the effectiveness of Port State Control (PSC) inspections, using DBN to assess ship conditions and risk levels. Their analysis of inspection records highlighted the importance of dynamic inspection regimes in reducing maritime accident probabilities. Zhu et al. (2024) integrated System Theoretic Process Analysis (STPA) with DBN to assess convoy operations in Arctic ice-covered waters. Their study identified sea ice and communication failures as pivotal risk factors and provided a detailed evaluation of system-level risks during operational stages. Similarly, Hu et al. (2023) applied DBN to assess piracy risks along the Maritime Silk Road, revealing temporal and spatial risk patterns such as heightened vulnerabilities in the Gulf of Guinea and the Gulf of Aden. Additionally, Liu et al. (2024b) employed DBN to study navigation risks in the Arctic Northeast Passage, focusing on factors like ice conditions, ship speed, and navigation expertise. Both studies underscored the ability of DBN to model region-specific maritime risks with high accuracy and relevance. Fan et al. (2024a) proposed a novel DBN-based framework for assessing risk in maritime trade routes, particularly emphasising dynamic risk performance evaluation over time. Their approach incorporates synthetic minority over-sampling and the edited nearest neighbour method to address imbalanced accident data. The gradient descent algorithm and Markov chain model further enhance the framework's predictive capabilities. The case study on the Indian Ocean route reveals significant insights into the temporal dynamics of risks, such as terrorism and piracy, showcasing the framework's utility for stakeholders in prioritising and mitigating vulnerabilities. A DBN model, combined with the FRAM, was developed to assess collision risk during ship pilotage operations. The Dempster-Shafer (D-S) evidence theory and the Markov model were employed to establish the prior probabilities and configure the transition probability table, respectively.

Alongside environmental factors, ship traffic density was incorporated as a novel dynamic variable, updated using historical AIS data (Guo et al., 2023). Li et al. (2022d) developed a navigational risk performance model for LNG tanker ships operating in Arctic waters using a DBN. This model incorporates variable data from marine meteorological analysis, shipborne sensors, and expert knowledge to enhance accuracy. By utilising the DBN model, the inference of collision risk performance for LNG carriers, along with the identification of key influential factors, was conducted over a 24-hour period. The primary risks in Arctic summer waters are posed by difficult-to-detect obstacles such as icebergs and reefs within navigational channels. To address these dynamic risks, a State Transition Matrix based on the Markov process was employed as a Transient Probability Table (TPT), enabling the calculation of updated prior probabilities for influential factors across time slices. Beyond assessing the dynamic risks of surface ships, the study also examined the navigation safety of underwater vehicles by applying a DBN approach, which combined structure and parameter learning with the D-S evidence theory, under a specified route plan (Li et al., 2022b). The DBN also demonstrated significant capability in integrating both qualitative and quantitative data from daily records over a 14-day period. Rothmund et al. (2022) developed a novel collision avoidance strategy by utilising the DBN method to predict the intended direction of target ships. The strategy takes into account real-time behaviours, such as ship speed and manoeuvrability, and generates potential paths. These paths are then scored based on their likelihood of being safe, expressed as a percentage. Additionally, the approach incorporates the encounter logic of the COLREG, particularly for open sea scenarios.

The applications of DBN have been extensively explored across various domains in maritime risk assessment, demonstrating strong capabilities in modelling dynamic and complex systems. The reviewed studies highlight the versatility of DBN in addressing a wide range of challenges, including environmental hazards, Arctic navigation risks, and socio-economic disruptions such as the COVID-19 pandemic. Furthermore, the integration of advanced techniques such as synthetic minority over-sampling, Markov chain models, and evidence theory has enhanced the precision and applicability of DBN frameworks. Despite these advancements, a significant gap remains in the direct application of DBN modelling to ship-to-ship encounter scenarios using AIS data. While DBN has been successfully employed in areas such as ship-to-offshore collisions, Arctic navigation risks, and convoy operations, its potential for real-time dynamic collision risk assessment using AIS data remains largely unexplored. Addressing this gap could lead to significant improvements in maritime safety, particularly in high-traffic and high-risk zones, by providing data-driven insights for collision avoidance and navigational decision-making.

2.3. Research gaps

A comprehensive critical literature review has identified key gaps in ship-to-ship collision risk analysis, which are addressed through the DBN-based model developed in this study.

(1) Reliability of AIS data in collision risk analysis for real-time risk prediction.

Numerous candidate models have been proposed for ship-to-ship collision risk assessment, assuming that AIS data is perfectly recorded at one-minute intervals without critically evaluating its reliability and robustness. However, AIS data is often noisy in real-world scenarios, contains missing information at certain intervals, and may deviate from expected trajectory patterns. To address these challenges, the DBN-based model developed in this study leverages the strengths of a transition mechanism grounded in Markov chain analysis, effectively handling data inconsistencies while enhancing predictive accuracy.

(2) Limitations of traditional measurement factors.

Advanced models typically incorporate Euclidean-based measurement factors such as DCPA, TCPA, and relative distance. In this study, insights drawn from real-world collision accidents revealed that, during normal manoeuvring actions, the relative changes in

these factors varied gradually over time. However, just before the point of collision, both ships exhibited evasive actions, resulting in sudden and significant variations in speed ratio and relative bearing. Recognising their significance, these novel indicators have been integrated into the DBN-based model, alongside traditional risk assessment factors, to enhance its predictive capabilities.

(3) Lack of a real-time causation probability framework in ship-to-ship collision risk models.

Most existing methods adopt a geometry-based approach, where the CRI is typically defined as a function of memberships. However, no prior research has applied a causation probability framework that defines risk through discrete levels based on the AIS data. This study establishes mutual relationships between influential factors to develop a dynamic collision risk model, marking the first application of causation probability methods in conjunction with geometric probability parameters. This approach represents a novel contribution to maritime collision risk assessment.

(4) Applicability across different scenarios and vessel types.

The adaptability of collision risk assessment models across different navigational scenarios often necessitates parameter tuning, which makes practical implementation challenging. Additionally, AIS data typically requires pre-processing, such as data cleansing, before being used in these models. However, the DBN-based model proposed in this study is designed to be straightforward and flexible, allowing it to be applied to various vessel types without extensive parameter adjustments, even when using raw AIS data.

(5) Integration of macro and micro-scale perspectives in collision risk assessment.

The literature analysis reveals a significant gap in integrating macro-scale (causation-based) and micro-scale (geometric-based) approaches in maritime collision risk assessment. Geometric-based models offer a detailed, micro-scale evaluation of collision risks in ship-to-ship encounters, while causation-based models provide a broader perspective by incorporating ship-specific, system-related, and environmental factors. This study bridges this gap by applying a causation probability approach to provide a micro-scale evaluation of ship-to-ship encounters. Moreover, the model can be extended to incorporate macro-scale factors, providing a more holistic and dynamic framework for assessing ship-to-ship collision risk in the maritime domain.

3. Methodology

This study integrates geometric and causation probability approaches into a DBN model for real-time collision risk assessment. Section 3.1 presents an overview of the proposed methodology, while Section 3.2 describes the preprocessing of AIS data. Sections 3.3 and 3.4 then introduce the data-driven BN modelling and its extension into a DBN framework, respectively. Owing to the novelty of the

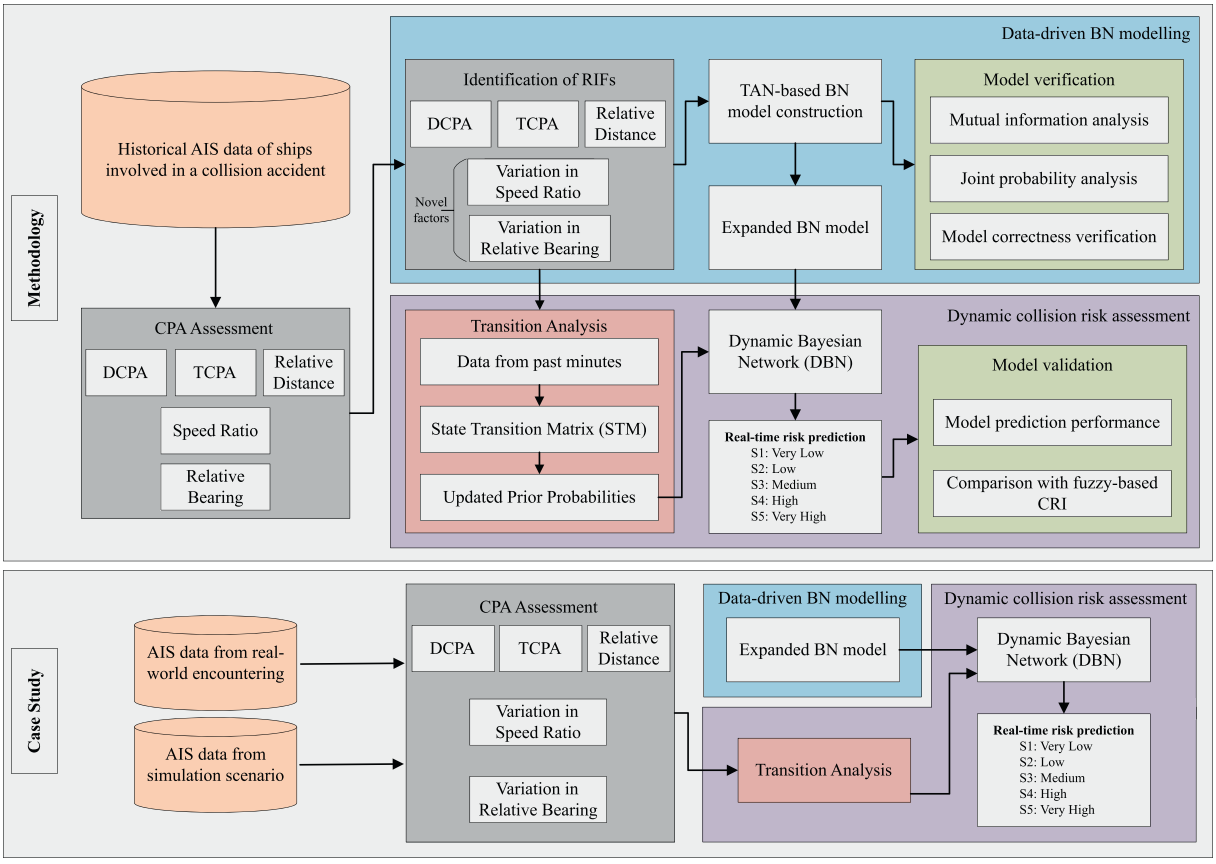

Fig. 1. Framework of dynamic collision risk assessment.

approach, Section 3.5 provides a systematic verification and validation analysis to demonstrate the robustness of the model.

3.1. Overview of the proposed method

The framework for dynamic ship collision risk assessment is illustrated in Fig. 1. Historical AIS data from a real ship-to-ship collision accident is utilised for data-driven BN modelling. First, raw AIS data undergoes CPA assessment to calculate Euclidean-based parameters, after which the processed data in RIF format is employed to construct a fully structured BN. The BN model is then expanded into a temporal space to enable dynamic collision risk assessment. In dynamic modelling, at each time slice, CPA-evaluated historical data is analysed with a Markov chain model to update the Prior Probability Distribution (*PPD*). The DBN model is then achieved by integrating the updated *PPD* with the expanded BN model. Finally, the collision risk between the OS and TS (s) is predicted in terms of categorised risk levels. While DBN has been extensively applied in maritime safety research, this study uniquely applies a DBN-based framework to real-time ship-to-ship collision risk assessment using raw AIS data, which has not been explicitly addressed in prior works. The model is rigorously verified through sensitivity analysis and validated using prediction performance across different stages of implementation.

In case studies, both real AIS data from near-miss encounters and simulation-based AIS data from multi-ship encounters are utilised for real-time experiments. The data is first processed through CPA assessment, where novel factors are directly incorporated for dynamic risk assessment. Transition modelling of the processed AIS data from preceding minutes is then performed at each time slice to update the *PPD*. The *PPD* is used as input in the expanded BN model, configured as a DBN, to assess the real-time collision risk between the OS and TS(s).

3.2. CPA assessment

Raw AIS data provides detailed positional and kinematic information for ships. In this study, the dataset includes longitude, latitude, speed, and course. While the data contains attributes of individual vessels, meaningful interactions must be extracted to enable accurate collision risk assessment. Furthermore, reliable evaluation requires a broader set of factors beyond the relative distance between the OS and TS. Specifically, this study adopts factors from the fuzzy-based CRI approach, which represents one of the most advanced methodologies for collision risk assessment: DCPA, TCPA, relative distance (D_R), relative bearing (θ_T), and speed factor (λ). Geometric calculations in ship encounter scenarios, as illustrated in Fig. 2, enable the derivation of DCPA, TCPA, D_R, θ_T, and relative velocity (V_R). The coordinates, velocity, and the course of the OS are denoted as $S_O(x_O,y_O)$, V_O, and φ_O, while those of the TS are $S_T(x_T,y_T)$, V_T, and φ_T. Additionally, a_T signifies the azimuth of the TS.

The DCPA and TCPA between the OS and TS are calculated as follows (Li & Pang, 2013):

$$\mathrm{DCPA} = D_R \sin(\varphi_R - a_T - \pi) \tag{1}$$

$$\mathrm{TCPA} = D_R \cos(\varphi_R - a_T - \pi)/V_R \tag{2}$$

The coordinates of both the OS and the TS can be used to derive the relative distance between them as follows:

$$D_R = \sqrt{(x_T - x_O)^2 + (y_T - y_O)^2} \tag{3}$$

The angle of relative velocity, denoted as φ_R, is measured with respect to the true north. The value of φ_R can be calculated using the following equations:

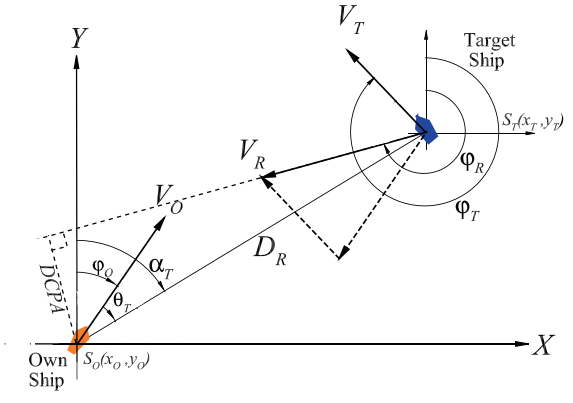

Fig. 2. Geometrical configuration of the two ships in an encounter.

$$\varphi_R = \begin{cases} \tan^{-1}(V_{Rx}/V_{Ry}), V_{Rx} \geq 0, V_{Ry} \geq 0 \\ \tan^{-1}(V_{Ry}/V_{Rx}) + 90, V_{Rx} \geq 0, V_{Ry} \leq 0 \\ \tan^{-1}(V_{Rx}/V_{Ry}) + 180, V_{Rx} \leq 0, V_{Ry} \leq 0 \\ \tan^{-1}(V_{Ry}/V_{Rx}) + 270, V_{Rx} \leq 0, V_{Ry} \geq 0 \end{cases} \tag{4}$$

Here, V_{Rx} and V_{Ry} are the components of the relative velocity on the x and y axes, respectively, and are calculated as:

$$\begin{cases} V_{Rx} = V_{Tx} - V_{Ox} \\ V_{Ry} = V_{Ty} - V_{Oy} \end{cases} \tag{5}$$

The velocity components of the OS and TS are calculated as:

$$\begin{cases} V_{Ox} = V_O sin\varphi_O \\ V_{Oy} = V_O cos\varphi_O \end{cases} \text{ and } \begin{cases} V_{Tx} = V_T sin\varphi_T \\ V_{Ty} = V_T cos\varphi_T \end{cases} \tag{6}$$

The V_R is obtained as:

$$V_R = \sqrt{{V_{Rx}}^2 + {V_{Ry}}^2} \tag{7}$$

The θ_T is the relative bearing obtained by:

$$\theta_T = a_T - \varphi_O \tag{8}$$

where a_T denotes the true bearing of the TS, it is calculated using the following equality scheme (Hu et al., 2020).

$$a_T = \begin{cases} \tan^{-1}(x_{OT}/y_{OT}), x_{OT} \geq 0, y_{OT} \geq 0 \\ \tan^{-1}(x_{OT}/y_{OT}) + 180, x_{OT} < 0, x_{OT} < 0 \\ \tan^{-1}(x_{OT}/y_{OT}) + 180, x_{OT} \geq 0, y_{OT} < 0 \\ \tan^{-1}(x_{OT}/y_{OT}) + 360, x_{OT} < 0, y_{OT} \geq 0 \end{cases} \tag{9}$$

Here, x_{TO} and y_{OT} are the distances of the OS and TS on the x and y axes, respectively, and are calculated as:

$$\begin{cases} x_{OT} = x_T - x_O \\ y_{OT} = y_T - y_O \end{cases} \tag{10}$$

Finally, the λ (i.e., the speed ratio) is obtained by:

$$\lambda = \frac{V_O}{V_T} \tag{11}$$

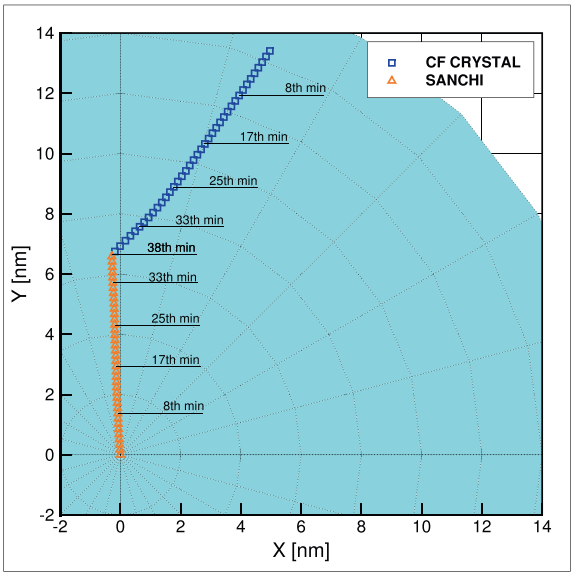

Fig. 3. Trajectories of SANCHI and CF CRYSTAL before the collision accident.

3.3. Data-driven BN modelling

3.3.1. Data aggregation and processing

Historical AIS data from two vessels involved in an accident (e.g., SANCHI and CF CRYSTAL in the East China Sea at 19:50 on January 6, 2018, as illustrated in the generic methodology) have been collected. The dataset begins at 19:11, when the initial relative distance between the ships was approximately 14 nautical miles (nm). The AIS data were processed following the CPA assessment procedure described in Section 3.2 to construct a dataset covering the primary variables. Fig. 3 presents the trajectories of SANCHI and CF CRYSTAL before the collision.

3.3.2. Identification of collision RIFs

In conventional CRI research, the most comprehensive models typically include variables such as DCPA, TCPA, relative distance, relative bearing, and speed factor. Similarly, collision-related RIFs in this study are derived primarily from CPA-assessed AIS data. In addition, relative bearing and speed ratio are further analysed to capture evasive manoeuvre patterns, as empirical observations reveal significant fluctuations in these variables just before collision occurrence. Instead of directly incorporating relative bearing and speed ratio, their temporal variations are modelled as influential factors in the BN construction.

$$\Theta_T^{(t)} = \left|{\theta_T}^{(t+1)} - {\theta_T}^{(t)}\right|,\ t = 1, \cdots, n-1 \tag{12}$$

$$\dot{\Theta}_T = \frac{\Theta_T}{\max(\Theta_T) - \min(\Theta_T)}$$

$$\Lambda_T^{(t)} = \left|{\lambda_T}^{(t+1)} - {\lambda_T}^{(t)}\right|,\ t = 1, \cdots, n-1 \tag{13}$$

$$\dot{\Lambda}_T = \frac{\Lambda_T}{\max(\Lambda_T) - \min(\Lambda_T)}$$

Here, n is the length of the time series from the beginning to the collision occurrence point, the Θ_T defines the relative difference of relative bearings between the time steps. The $\dot{\Theta}_T$ is the normalised expression of the variation in relative bearing. The same formulation is produced for the variation in speed factor ($\dot{\Lambda}_T$) in Eq. (13). To sum up, the processed dataset consists of five RIFs, which are DCPA, TCPA, D_R, $\dot{\Theta}_T$, and $\dot{\Lambda}_T$. The threshold values for the states of the RIFs are defined below.

At the final time (19:50), the collision occurred, and the target node representing collision risk was assigned a value of 1, whereas the initial collision risk was defined as 0. Intermediate data points were linearly interpolated, and the threshold values for the states of the collision risk node were determined to ensure an equal distribution of data across each state. For the influential factors, different strategies were adopted depending on the availability of domain knowledge (e.g. established regulations and best practices) or empirical references. The relative distance thresholds were defined directly from the critical distances outlined in COLREG, specifically 1 nm, 3 nm, 6 nm, and 10 nm, which are commonly recognised as decision-making limits. The DCPA states were configured using Eq. (A-1) in the Appendix A, where the critical distances were calculated as a function of relative bearing (θ_T) according to the fuzzy-based CRI model. The resulting threshold values were set at 0.6, 0.75, 0.975, and 1.1 nm. Since TCPA is inherently related to DCPA, the corresponding TCPA values observed in the collision accident data were used to define the state thresholds for this factor. In contrast, for the variation in relative bearing and the speed ratio, no domain-specific or empirical thresholds were available. Therefore, these states were discretised using an equal-interval binning approach, consistent with the equal-distribution criterion used for the collision risk target node. A comprehensive summary of the threshold values for all RIFs is provided in Table 2.

3.3.3. BN structure learning

Traditional and advanced mathematical models calculate the collision risk index using variables such as DCPA, TCPA, relative distance, relative bearing, and speed ratio. From a risk assessment perspective, these models typically calculate the index by directly utilising these variables without accounting for their interdependencies. For instance, in CPA assessment, the computation of DCPA and TCPA relies on information about relative distance, velocity, and bearing. Therefore, understanding these dependencies and integrating them into risk predictions allows for a more comprehensive assessment of collision risk.

A BN is a Directed Acyclic Graph (DAG) that encodes conditional dependencies between parent and child nodes, where Conditional Probability Tables (CPT) are generally constructed from expert knowledge, logical reasoning, or data-driven techniques. In this study,

Table 2
Threshold values for the states of the RIFs.

	S1	S2	S3	S4	S5
Collision Risk	[0.00, 0.18]	[0.18 to 0.39]	[0.39, 0.61]	[0.61, 0.82]	[0.82, 1.00]
Variation in Relative Bearing	[0.000, 0.013]	[0.013, 0.029]	[0.029 to 0.044]	[0.044 to 0.210]	[0.210 to 1.000]
Variation in Speed Ratio	[0.000, 0.004]	[0.004, 0.008]	[0.008, 0.012]	[0.012, 0.140]	[0.140, 1.000]
Relative Distance [nm]	[10, +∞]	[6, 10]	[3, 6]	[1, 3]	[0, 1]
TCPA [hour]	[0.450, +∞]	[0.265, 0.450]	[0.140, 0.265]	[0.050, 0.140]	[0.000, 0.050]
DCPA [nm]	[1.100, +∞]	[0.975, 1.100]	[0.750, 0.975]	[0.600, 0.750]	[0.000, 0.600]

a data-driven approach is employed to train and construct CPT using processed AIS data. Among various BN algorithms, such as Naïve Bayes Networks (NBN), the Tree-Augmented Naïve Bayes (TAN) approach is selected as a structural learning algorithm for its ability to capture mutual relationships among parent nodes while preserving dependencies between parent and child nodes. This study pioneers the application of a TAN-based BN model for ship-to-ship collision risk assessment using historical AIS data from a real collision accident.

$$I_P(X_i, X_j|C) = \sum_{x_{ii}, x_{ji}, c_i} P(x_{ii}, x_{ji}, c_i) \log \frac{P(x_i, x_j|c_i)}{P(x_{ii}|c_i)P(x_{ji}|c_i)} \tag{14}$$

where I_P defines the conditional mutual information, x_{ii} is the i-th state of the attribute variable X_i, x_{ji} is the i-th state of the attribute variable X_j, and c_i is the i-th state of the class variable C. In this research, collision is designated as the target node (class variable) to analyse the influence of various factors on the probability of different risk levels.

After configuring the TAN network structure, the CPT is established by incorporating the database into the TAN model. The resulting data-driven BN model is illustrated in Fig. 4.

3.4. Dynamic collision risk assessment

3.4.1. DBN model implementation

The DBN fundamentally consists of a series of time slices, carrying a Bayesian network reasoning at each. The PPD at each time slice varies depending on the defined TPT. The collision risk detection is defined by Eq. (15), where $P(Si)^t$ corresponds to the belief results of the Bayesian network reasoning in terms of the risk levels at each time slice. CPT represents the conditional probabilities already constructed by the data-driven technique. $\otimes$ is the operator for the Bayesian reasoning. PPD^t_{k+1} represents the probability distribution vector at time t, where t is a discrete time index. PPD^t_{k+1} is calculated iteratively (Eq. (16)). This iterative process propagates the state probabilities forward over time according to the transition matrix STM^t.

$$P(Si)^t = PPD^t_{k+1} \otimes CPT \tag{15}$$

$$PPD^t_{k+1} = PPD_j \times STM^t \text{ for } k = 1, 2, 3, \cdots, N-1 \tag{16}$$

PPD_1 is the initial distribution vector at time t, which is typically initialised based on statically obtained prior probabilities (see Eq. (18)). The CPA assessed past minutes of AIS data is taken as time series sequence at time t. N presents the number of elements in the sequence.

Let v_j be the value at the k-th index of the sequence. The states (S_i) can be defined as:

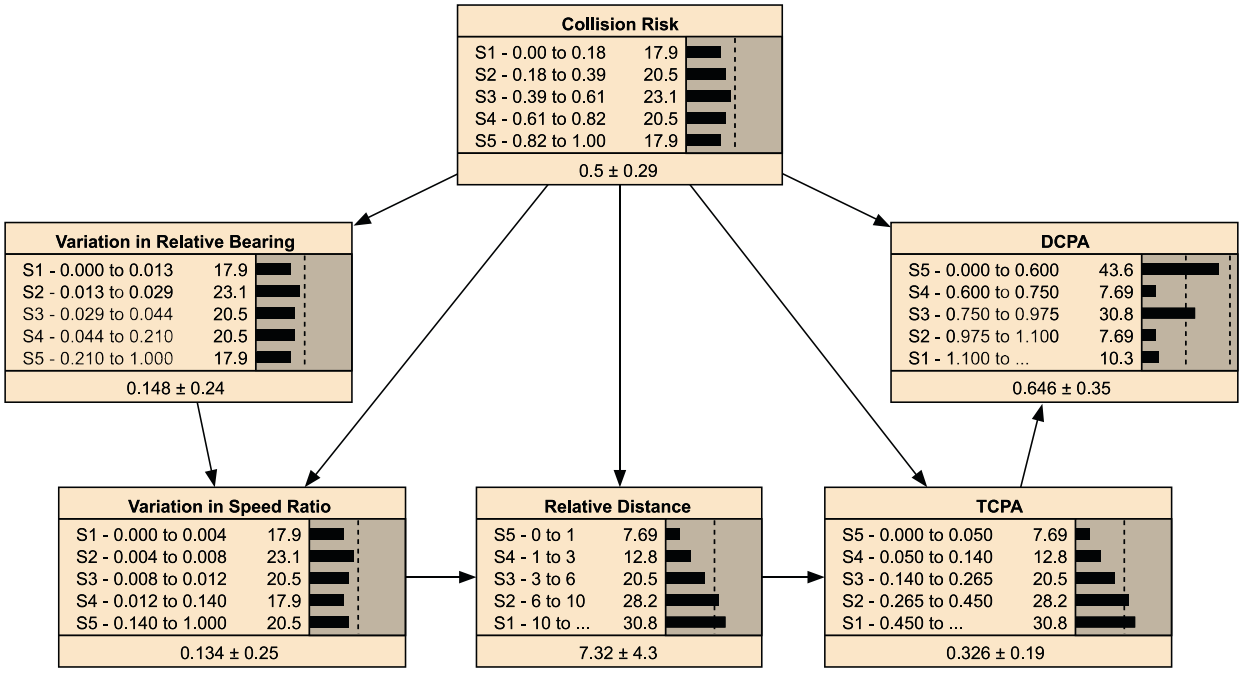

Fig. 4. The constructed TAN-based BN model.

$$S_i = \{v_k | T_{i-1} < v_k \leq T_i\}, \text{for } i = 2, 3, 4 \tag{17}$$

with including the S_1 and S_5:

$$S_1 = \{v_k | v_k \leq T_1\}, S_5 = \{v_k | T_4 < v_k\}$$

T_i represents the threshold values for the classification of S_i states.

PPD_1 for each state is calculated as:

$$PPD_1(S_i) = \frac{\sum_{j=1}^{N} I(v_k \in S_i)}{N}, i = 1, \cdots, 5 \tag{18}$$

$I(v_k \in S_i)$ is the indicator function that returns 1 if v_k belongs to the state S_i, and 0 otherwise.

3.4.2. STM calculation

The employed DBN model is built upon the framework of a static data-driven BN and requires an appropriate TPT selection based on the problem and relevant dynamic factors.

AIS data and its CPA assessment can be classified as deterministic data, as they are obtained from quantified observations. However, due to the inherently noisy nature of AIS data, predicting collision risk probability solely based on instantaneous AIS information can lead to high uncertainty. To mitigate this issue, CPA-assessed AIS data from previous minutes is utilised to extract more reliable information, which is then incorporated as the *PPD* for a given state. Since the state probability distribution evolves over time, the Markov chain method effectively addresses the associated challenges. Fig. 5 represents the Markov transition framework depicting five states of dynamic risk factors. The S_1, S_2, S_3, S_4, and S_5 present the five states, and γ, ζ, η, τ, and φ represent the probability of transitions between the states.

$I(v_{k+1} \in S_n)$ is the indicator function that returns 1 if v_{k+1} belongs to state $S_n, n = 1, \cdots, 5$ and 0 otherwise at time $k+1$ for a certain state at time k. The probabilities of transitions are calculated as:

$$\gamma_{1n} = \frac{\sum_{k=1}^{N-1} I(v_{k+1} \in S_n)}{\sum_{k=1}^{N-1} I(v_k \in S_1)} \tag{19}$$

$$\zeta_{2n} = \frac{\sum_{k=1}^{N-1} I(v_{k+1} \in S_n)}{\sum_{k=1}^{N-1} I(v_k \in S_2)} \tag{20}$$

$$\eta_{3n} = \frac{\sum_{k=1}^{N-1} I(v_{k+1} \in S_n)}{\sum_{k=1}^{N-1} I(v_k \in S_3)} \tag{21}$$

$$\tau_{4n} = \frac{\sum_{k=1}^{N-1} I(v_{k+1} \in S_n)}{\sum_{k=1}^{N-1} I(v_k \in S_4)} \tag{22}$$

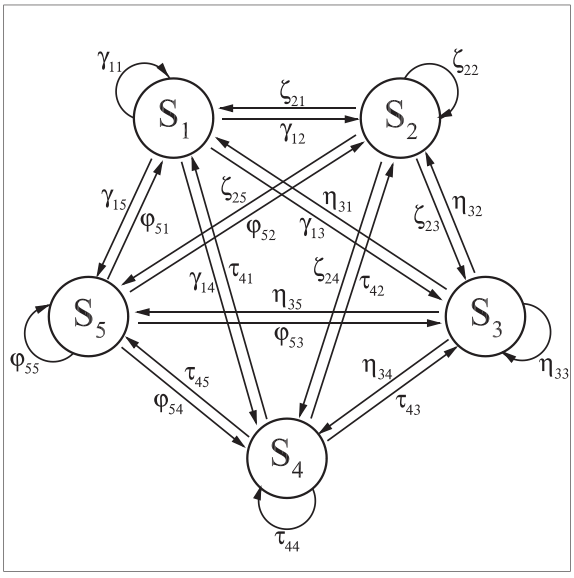

Fig. 5. Markov transition framework between the states.

$$\varphi_{5n} = \frac{\sum_{k=1}^{N-1} I(v_{k+1} \in S_k)}{\sum_{k=1}^{N-1} I(v_k \in S_5)} \tag{23}$$

The STM of a certain risk factor can be configured as follows.

$$STM = \begin{bmatrix} \gamma_{11} & \gamma_{12} & \gamma_{13} & \gamma_{14} & \gamma_{15} \\ \zeta_{21} & \zeta_{22} & \zeta_{23} & \zeta_{24} & \zeta_{25} \\ \eta_{31} & \eta_{32} & \eta_{33} & \eta_{34} & \eta_{35} \\ \tau_{41} & \tau_{42} & \tau_{43} & \tau_{44} & \tau_{45} \\ \varphi_{51} & \varphi_{52} & \varphi_{53} & \varphi_{54} & \varphi_{55} \end{bmatrix} \tag{24}$$

To extract a meaningful transition pattern from the data, the STM is constructed using AIS data from the eight-minute period preceding a specific time, *t*. This approach provides a robust framework for dynamic evaluation, even when some data deviate from the expected pattern. To determine an appropriate time window for the STM module, a series of experiments was conducted using various durations: five, six, eight, ten, and twelve minutes. These durations were evaluated on a real-world collision scenario involving the vessels CF CRYSTAL and SANCHI, in which the model was repeatedly executed to examine how the time window affects the dynamics of collision risk prediction. The results indicate that, while the numerical values of the predicted collision risk vary slightly with different time windows, the corresponding risk level categories (e.g., High, Very High) remain consistent (see Fig. B1 in the Appendix). This finding suggests that the model's output is not highly sensitive to changes in the time window in terms of risk classification. Nevertheless, it was observed that shorter time windows tend to result in abrupt transitions between risk levels, potentially leading to unstable or overly reactive behaviour in real-time applications. In contrast, longer time windows introduce delays in updating the risk level, reducing the model's ability to capture rapid changes in ship encounter dynamics. Balancing these trade-offs, an eight-minute window was selected as it provides an effective compromise between temporal stability and responsiveness in dynamic maritime navigation scenarios. The STM captures the probabilistic transitions between different states over time, allowing for a more reliable assessment of collision risk. To ensure continuous adaptation to changing conditions, the STM is iteratively updated, and this updated matrix is then used to compute the *PPD* at each time slice. For instance, during the voyage between SANCHI and CF CRYSTAL, the STM for the 17th minute is constructed using CPA-assessed data as a time sequence from the preceding eight minutes. In this case, all DCPA values in the time sequence range between 0.750 and 0.975 nm, leading to no transitions and resulting in the system consistently remaining in state S3 during the observation period. (see Fig. 6(a)). The initial probability distribution for TCPA is 0.29 for state S1 and 0.71 for state S2. After evaluating the transitions, the probability of state S1 reduces to 0, while the probability of state S2 increases to 1. This shift indicates a clear trend in the temporal evolution of TCPA, highlighting the influence of past observations on future state estimations.

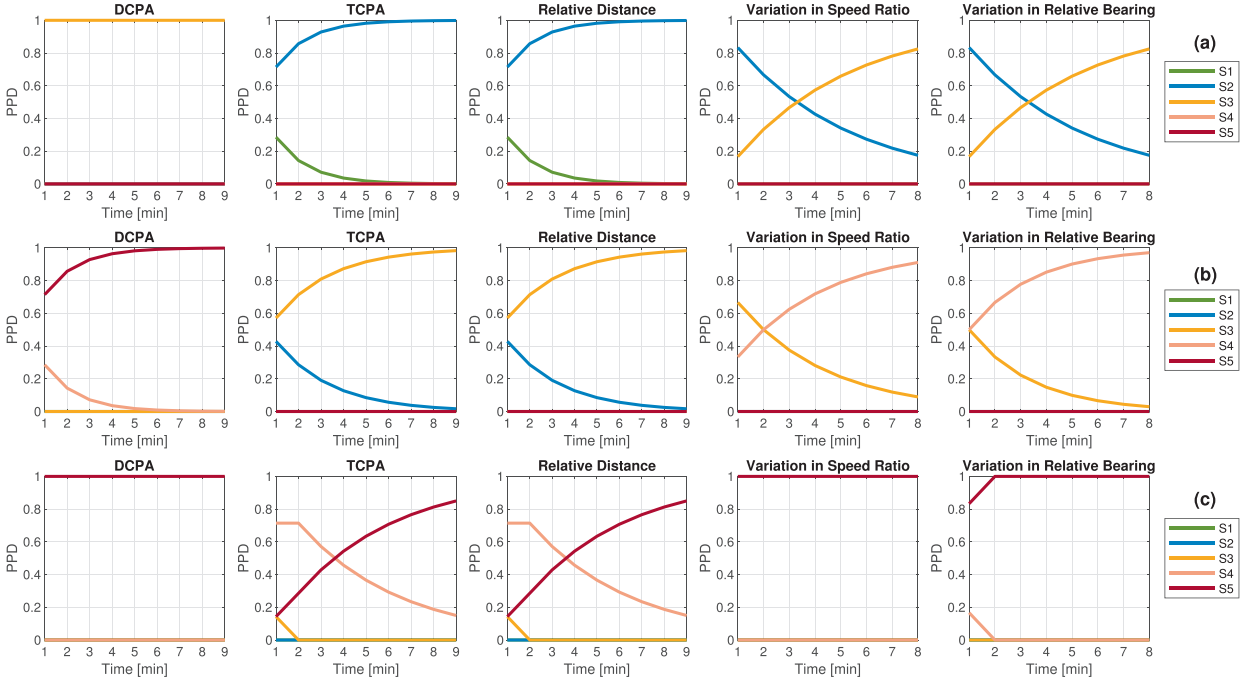

Fig. 6. State transitions of the RIFs at 17th(a), 27th(b), and 37th(c) minutes.

Further details of state transitions for relative distance, variation in speed ratio, and relative bearing are presented in the same row of Fig. 6(a). These parameters play a pivotal role in capturing the dynamic interactions between vessels and are key indicators of evasive manoeuvres or risk escalation. Additionally, the evolution of state levels over time is illustrated in Fig. 6(b) and Fig. 6(c) for the 27th and 37th minute marks, respectively. These visualisations provide insight into how state probabilities change as new information becomes available, reinforcing the effectiveness of the STM in modelling real-time collision risk dynamics.

Using the initial probabilities defined in Eq. (18) and the STM from Eq. (24), the prior probabilities are iteratively updated based on the recursive formulation in Eq. (16). These updated probabilities serve as inputs for predicting the level of collision risk, leveraging the CPT derived from a data-driven BN model. The state transitions exhibit smooth and continuous dynamics, facilitating stable and reliable collision risk predictions. This stability is particularly beneficial in maritime risk assessment, where abrupt fluctuations could lead to misleading interpretations of navigational hazards. Furthermore, the Markov transition framework effectively captures the temporal dependencies within the time series, ensuring strong coherence across sequential states. Even in the presence of noisy AIS data, this approach maintains consistency and robustness, enhancing the model's ability to provide accurate risk assessments under real-world conditions.

3.4.3. Computational tools

The data-driven BN model was developed using Netica software, whose core libraries are written in C. Although Netica supports DBN applications by extending BN into the temporal domain, its functionality is primarily suited to problems with a limited number of time slices (e.g., yearly or monthly analyses). For real-time applications involving a large number of time slices, manual intervention within Netica becomes impractical and time-consuming. To address this limitation, Netica-J was integrated with MATLAB through Netica's Application Programming Interface (API). This integration allows the DBN structure constructed in Netica to be executed seamlessly in MATLAB, where both the prior probabilities (derived from the state transition matrix, STM) and the initial probability distributions are calculated. Consequently, all inference and updating processes are carried out consistently within MATLAB. In the context of ship-to-ship collision risk assessment, raw AIS data from both the OS and the TS are supplied to the DBN model, which evaluates collision risk in discrete levels at sub-second intervals.

3.5. Model verification and validation

This section presents the verification and validation of the constructed BN model. Sections 3.5.1 and 3.5.2 conduct mutual information and joint probability analyses to examine underlying dependencies and model consistency, forming the basis for correctness verification in Section 3.5.3. The prediction performance of the DBN is then evaluated in Section 3.5.4, followed by a comparative assessment against an advanced fuzzy-based CRI model in Section 3.5.5 to benchmark its relative performance.

3.5.1. Mutual information

The five RIFs are evaluated through their mutual information values shared with the target node 'Collision Risk' as presented in Table 3. A higher mutual information value indicates a stronger influence of the corresponding RIF on the 'Collision Risk' outcomes. As shown in Table 3, the RIFs significantly impact the target node, with the highest influence attributed to the 'Variation in Relative Bearing', followed by the 'Variation in Speed Ratio', 'Relative Distance', 'TCPA', and 'DCPA'.

3.5.2. Joint probability analysis

After analysing the mutual information shared between the variables, the RIFs are further examined to understand the model's behaviour under various joint conditions. State S1 corresponds to a 'Very Low' level of the target node, 'Collision Risk', while State S5 represents a 'Very High' level. The state descriptions and the initial probability distribution of 'Collision Risk' are presented in the first row of Table 4.

Each parent node also consists of five distinct states; however, their categorisation differs from that of the target node. The states of DCPA are assigned based on dimensional values, where S1 represents a greater distance, while S5 corresponds to a shorter distance. Similarly, the states of TCPA follow a time-based distribution, with S1 indicating a longer time until the closest point of approach and S5 a shorter time. The states of 'Relative Distance' are also distributed dimensionally, with S1 representing distances greater than 10 nm, while S5 corresponds to distances below 1 nm. Meanwhile, the 'Variation in Speed Ratio' and 'Variation in Relative Bearing' are discretised based on transition intensity, where S1 represents minimal variation, while S5 signifies significant evasive manoeuvres at each time slice.

Table 3
Mutual information shared with "Collision Risk".

	Mutual Information	Percent	Variance of Beliefs
Collision Risk	2.3153	100.0	0.6374
Variation in Relative Bearing	2.1991	95.0	0.5889
Variation in Speed Ratio	2.0875	90.2	0.5389
Relative Distance	1.5711	67.9	0.2580
TCPA	1.5711	67.9	0.2580
DCPA	1.4213	61.4	0.2359

Table 4
Joint probability results.

	Collision Risk				
	S1:Very Low	**S2:Low**	**S3:Medium**	**S4:High**	**S5:Very High**
Initial Values	17.9	20.5	23.1	20.5	17.9
DCPA					
S1	100.0	0.0	0.0	0.0	0.0
S2	100.0	0.0	0.0	0.0	0.0
S3	0.0	66.7	33.3	0.0	0.0
S4	0.0	0.0	100.0	0.0	0.0
S5	0.0	0.0	11.8	47.1	41.2
TCPA					
S1	58.3	41.7	0.0	0.0	0.0
S2	0.0	27.3	72.7	0.0	0.0
S3	0.0	0.0	12.5	87.5	0.0
S4	0.0	0.0	0.0	20.0	80.0
S5	0.0	0.0	0.0	0.0	100.0
Relative Distance					
S1	58.3	41.7	0.0	0.0	0.0
S2	0.0	27.3	72.7	0.0	0.0
S3	0.0	0.0	12.5	87.5	0.0
S4	0.0	0.0	0.0	20.0	80.0
S5	0.0	0.0	0.0	0.0	100.0
Variation in Speed Ratio					
S1	100.0	0.0	0.0	0.0	0.0
S2	0.0	88.9	11.1	0.0	0.0
S3	0.0	0.0	100.0	0.0	0.0
S4	0.0	0.0	0.0	100.0	0.0
S5	0.0	0.0	0.0	12.5	87.5
Variation in Relative Bearing					
S1	100.0	0.0	0.0	0.0	0.0
S2	0.0	88.9	11.1	0.0	0.0
S3	0.0	0.0	100.0	0.0	0.0
S4	0.0	0.0	0.0	100.0	0.0
S5	0.0	0.0	0.0	0.0	100.0

To evaluate the influence of each RIF, an individual state is assigned a prior probability of 100 %, and the model's prediction results are recorded in Table 4. For example, when DCPA is in state S1, the probability of 'Collision Risk' being in S1 is 100 %, while the probabilities for S2, S3, S4, and S5 remain 0 %. A similar pattern is observed when DCPA is in state S2. However, when DCPA is in state S5, representing a distance of less than 0.6 nm, the corresponding state probabilities for 'Collision Risk' are 0.0 % for S1, 0.0 % for S2, 11.8 % for S3, 47.1 % for S4, and 41.2 % for S5.

This process is repeated for each RIF, setting each state to 100 % one at a time, and the resulting predictions for 'Collision Risk' are documented in Table 4. This joint probability analysis provides insight into how different states of each RIF influence the 'Collision Risk', identifying the conditions that contribute most significantly to increased collision probability.

3.5.3. Model correctness verification

The fully structured BN model requires further verification, particularly in terms of its sensitivity to slight variations in influential factors. This part examines two specific theorems to assess the model's response. The first theorem posits that the model's response should exhibit a consistent trend when influential factors are slightly increased or decreased. The second theorem asserts that the model's response should change gradually, either increasing or decreasing, when each influential factor is adjusted individually (Li et al., 2023b; Zhang et al., 2013).

To test these theorems, each influential factor was increased by 2 %. The most pivotal state of the RIFs for the corresponding states

Table 5
Corresponding changes in collision risk states after a minor increase in RIFs.

DCPA		–	+ 2 %	+ 2 %	+ 2 %	+ 2 %	+ 2 %
TCPA		–	–	+ 2 %	+ 2 %	+ 2 %	+ 2 %
Relative Distance		–	–	–	+ 2 %	+ 2 %	+ 2 %
Variation in Speed Ratio		–	–	–	–	+ 2 %	+ 2 %
Variation in Relative Bearing		–	–	–	–	–	+ 2 %
Collision Risk	**S1**	17.9	19.9	21.2	22.4	24.4	26.4
	S2	20.5	21.9	22.8	23.7	25.5	27.3
	S3	23.1	25.1	26.6	28.1	30.1	32.1
	S4	20.5	21.5	23.2	25.0	27.0	29.0
	S5	17.9	18.8	20.8	22.7	24.6	26.6

of 'Collision Risk' had already been identified through joint probability analysis. Each pivotal state was subsequently increased by 2 %, and the resulting variation in the 'Collision Risk' state was recorded. For instance, the initial probability of state S1 in 'Collision Risk' was 17.9 %. Table 4 illustrates that the most pivotal state of the DCPA for S1 in 'Collision Risk' was also S1, leading to a 100 % probability prediction for this belief. Initially, the prior probability of DCPA's state S1 was 10.3 %, which increased to 12.3 %, resulting in a revised probability of 19.9 % for S1 in 'Collision Risk'. Next, the TCPA was analysed while maintaining the S1 state of DCPA at 12.3 %. The most pivotal state of TCPA for S1 in 'Collision Risk' was identified as S1, yielding a 58.3 % probability prediction. In the initial BN configuration, the prior probability of TCPA's state S1 was 30.8 %, which increased to 32.8 %, leading to an updated probability of 21.2 % for S1 in 'Collision Risk'. Subsequently, all remaining factors were slightly increased by 2 % for each state of the target node, with the results summarised in Table 5. The findings confirm that the model adheres to the conditions outlined in the theorems, demonstrating both slight increases in individual probability predictions and a cumulative upward trend in total probability estimates.

3.5.4. Model prediction performance

The predictive performance of the fully constructed BN model was assessed by implementing it as a DBN using transient prior probabilities. In this analysis, historical AIS data from a real collision accident were processed using the CPA method and subsequently utilised as real-time input for collision risk prediction. Fig. 7 presents the vessel trajectories at each minute, alongside the corresponding relative distance, DCPA, and TCPA values recorded throughout the voyage. As illustrated in the figure, the CPA parameters progressively decrease over time.

At each minute, prior probabilities are first updated based on the initial distribution and the unique STM derived from the preceding eight minutes. These updated probabilities are then integrated with the data-driven CPT through Bayesian reasoning to estimate the belief states of 'Collision Risk.' At the start of the analysis (minute 0), the relative distance, DCPA, and TCPA are recorded as 14.3 nm, 1.2 nm, and 0.64 h, respectively. According to the DBN model, the initial prediction for the collision risk of SANCHI concerning CF CRYSTAL falls within the 'Very Low' level (see Fig. 8). By the 8th minute, the 'Low' level of 'Collision Risk' becomes dominant. As time progresses, the risk level increases: at the 17th minute, the 'Medium' level becomes predominant, followed by the 'High' level at the 25th minute. By the 33rd minute, the 'Collision Risk' is classified as 'Very High', with a predicted probability of approximately 80 %. Five minutes later, the ships collide, with the probability of collision reaching 100 %, confirming the 'Very High' risk level.

3.5.5. Comparison with fuzzy-based CRI

One of the most advanced methods for CRI calculation is the fuzzy-based approach, which has been extensively utilised in collision risk assessment due to its ability to handle uncertainty and incorporate multiple factors (Seo et al., 2023; Abebe et al., 2021; Hu et al., 2020). This method integrates several key variables, including DCPA, TCPA, relative distance, speed ratio, and relative bearing, to systematically quantify collision risk. The CRI function in the fuzzy-based approach is formulated by defining membership functions and fuzzy inference rules, allowing for a flexible and adaptive risk assessment framework. It is defined as:

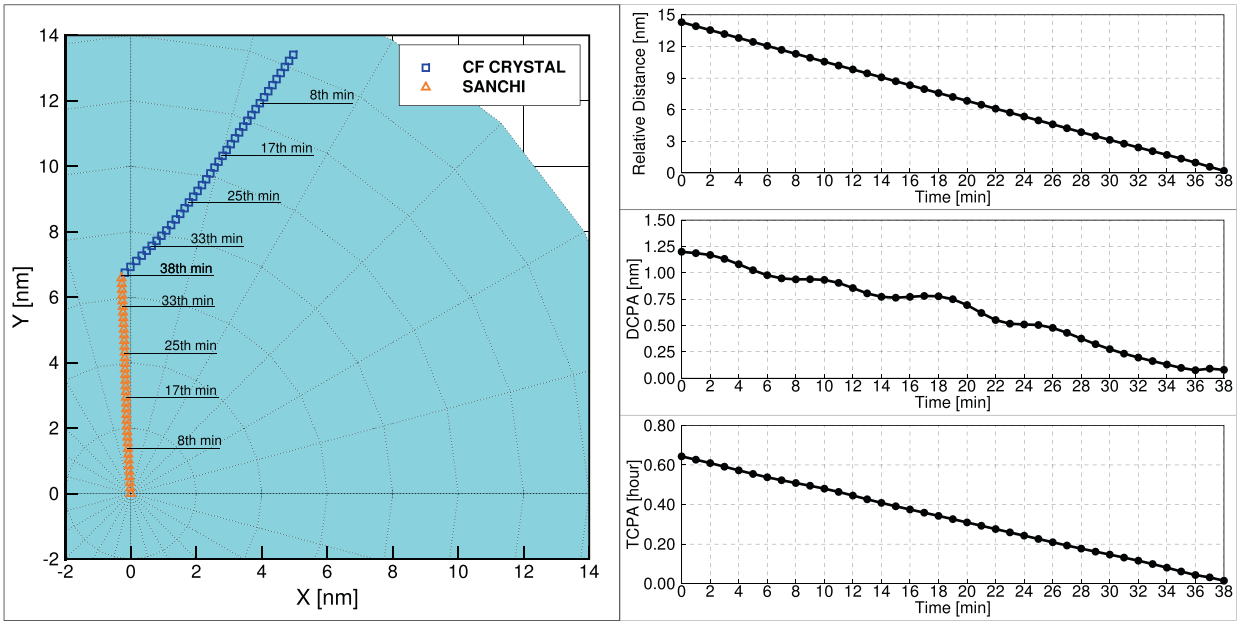

Fig. 7. Trajectories of SANCHI and CF CRYSTAL during the voyage together with the CPA assessed variables.

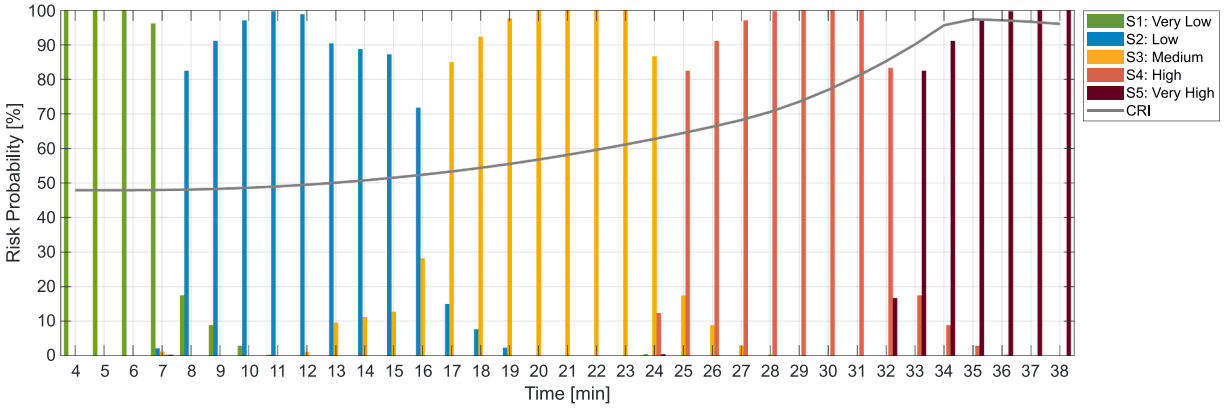

Fig. 8. Collision risk assessment with the DBN-based model.

$$CRI = W \bullet U = [w_{DCPA} w_{TCPA} w_{D_R} w_{\lambda} w_{\theta_T}] \begin{bmatrix} u_{DCPA} \\ u_{TCPA} \\ u_{D_R} \\ u_{\lambda} \\ u_{\theta_T} \end{bmatrix} \times 100 \tag{25}$$

Here, W represents the weight vector, while U denotes the membership vector, encompassing the membership functions for each variable. The weight values are adopted from existing studies (Seo et al., 2023; Hu et al., 2020) and are set as 0.400, 0.367, 0.133, 0.067, and 0.033, respectively.

The membership functions for DCPA, TCPA, relative distance, speed ratio, and relative bearing in the U vector are calculated as follows, respectively:

$$u_{DCPA} = \begin{cases} 1, & |DCPA| \le d_1 \\ 0.5 - 0.5 sin\left[\dfrac{\pi}{d_2 - d_1}\left(|DCPA| - \dfrac{d_2 + d_1}{2}\right)\right], & d_1 < |DCPA| \le d_2 \\ 0, & d_2 < |DCPA| \end{cases} \tag{26}$$

$$u_{TCPA} = \begin{cases} 1, & |TCPA| \le t_1 \\ \left(\dfrac{t_2 - |TCPA|}{t_2 - t_1}\right)^2, & t_1 < |TCPA| \le t_2 \\ 0, & t_2 < |TCPA| \end{cases} \tag{27}$$

$$u_{D_R} = \begin{cases} 1, & 0 \le D_R < D_1 \\ \left(\dfrac{D_2 - D_R}{D_2 - D_1}\right)^2, & D_1 \le D_R < D_2 \\ 0, & D_2 < D_R \end{cases} \tag{28}$$

$$u_{\lambda} = \frac{1}{1 + \frac{2}{\lambda\sqrt{\lambda^2 + 1 + 2\lambda sinC}}} \tag{29}$$

$$u_{\theta_T} = 0.5\left[cos(\theta_T - 19^{\circ}) + \sqrt{\frac{440}{289} + cos^2(\theta_T - 19^{\circ})}\right] - \frac{5}{17} \tag{30}$$

The unknown variables for each membership function are provided in the Appendix. In this study, the fuzzy-based CRI method is employed as a benchmark to systematically evaluate its performance against the proposed approach.

The results obtained from the fuzzy-based CRI model are illustrated in Fig. 8, where the grey line represents the computed risk index over time. As observed, the fuzzy-based model demonstrates a trend similar to that of the DBN-based model, exhibiting a consistent increase in CRI values as the collision scenario progresses. This close alignment between the two models provides further validation of the DBN-based approach, reinforcing its reliability in predicting collision risk levels.

Following this validation, the DBN model is further refined for application in real-world simulation case studies. These simulations enable a comprehensive evaluation of near-miss encounter scenarios and practical insights into maritime collision risk dynamics. By applying the DBN framework in realistic operational contexts, its effectiveness in predicting and mitigating collision risks can be demonstrated, supporting autonomous navigation and decision-support in maritime operations.

4. Case studies

Following verification and validation, the DBN model is evaluated using real-world AIS data in one-to-one encounter scenarios (Section 4.1) and simulation-based AIS data in multi-ship scenarios (Section 4.2). The results of these experiments are then discussed in Section 4.3.

4.1. Real-world encountering

According to the COLREG guidelines, three types of encounter situations are defined: head-on, crossing, and overtaking. These situations are determined based on the discretised regions around the reference ship, with a visual representation provided in Fig. 9.

The determination of which vessel is the stand-on vessel and which is the give-way vessel depends on the specific encounter situation, as outlined in the COLREG regulations. For example, as shown in Fig. 9, if the reference ship (OS) is positioned at the centre, and TS is approaching from the starboard crossing region, the OS must act as the give-way vessel. This is because the OS observes the TS on its starboard side, and according to COLREG, the OS is required to manoeuvre to avoid a collision. In addition, vessels are obligated to take action when certain distance thresholds are met. For head-on and crossing encounters, the relative distance between ships must be less than 6 nm, while for overtaking encounters, the threshold is reduced to 3 nm. Regarding encounter regions and distance criteria, real AIS data is collected under the assumption that vessels requiring action are within a maximum relative distance of 6 nm. The dataset includes a variety of encounter scenarios to reflect different real-world situations. While this data is historical, it is treated as real-time monitoring data when implemented in the DBN model. The model processes the raw data in a unified manner, without requiring any pre-processing, and can be easily adapted to any vessel. In the following subsections, the DBN model is assessed for different real encounter situations. The ship type information for both the OS and the TS is provided in Table 6. In addition, the initial parameter values, including speed, course, and position, are also presented. To simplify the figures, the latitude and longitude of the OS and TS are normalised with respect to the OS, which is assumed to be located at the origin (0, 0).

(1) Crossing encountering.

At the initial stage, Fig. 10 illustrates the TS positioned to the starboard of the OS. According to the COLREG regulations, the OS is required to take action toward its starboard side. This rule is applied by the OS, acting as the give-way vessel, while the TS, as the stand-on vessel, maintains its course. The DBN model predicts that the 'Medium' and 'High' states of 'Collision Risk' for the OS with respect to the TS each have a probability of around 40 % at the 4th minute. As the voyage progresses, the 'High' level of collision risk gradually increases, primarily due to a decrease in the TCPA and relative distance. While the Speed Ratio remains constant, the variation in relative bearing continues to increase, especially due to the manoeuvring actions taken by the OS. As shown in Fig. 11, by the 9th minute, the 'Very High' level of risk becomes dominant, with the probability approaching 65 %. After this point, the relative distance,

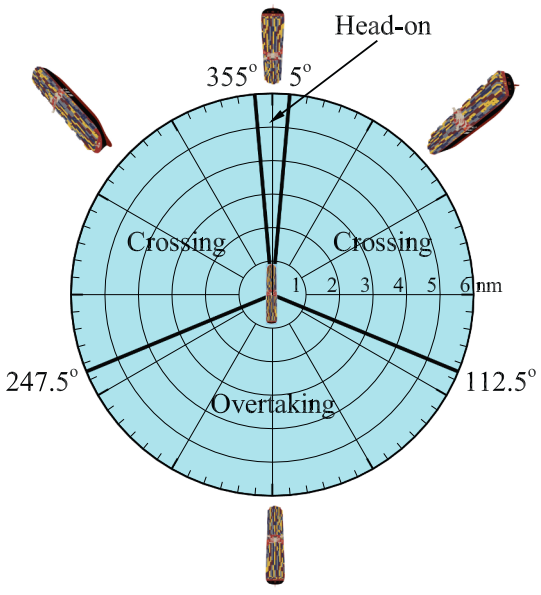

Fig. 9. Ship encounter regions defined by COLREG.

Table 6
Initial parameters of real-world encounter cases.

	OS					
Encountering Type	**Ship Type**	**Ship Length [m]**	**Latitude [nm]**	**Longitude [nm]**	**Speed [knot]**	**Course [deg]**
(1) Crossing	Container	148	0	0	13.67	14.44
	Cargo	147	0	0	9.62	202.06
(2) Head-on	Cargo	96	0	0	7.76	203.46
(3) Overtaking	Fishing	85	0	0	7.96	349.01
	TS					
Encountering Type	**Ship Type**	**Ship Length [m]**	**Latitude [nm]**	**Longitude [nm]**	**Speed [knot]**	**Course [deg]**
(1) Crossing	Cargo	90	1.782	5.399	11.47	203.91
	Container	255	−5.591	−0.996	14.16	107.12
(2) Head-on	Cargo	99	−1.914	−5.684	9.01	22.14
(3) Overtaking	Cargo	171	−1.733	−3.881	12.53	4.87

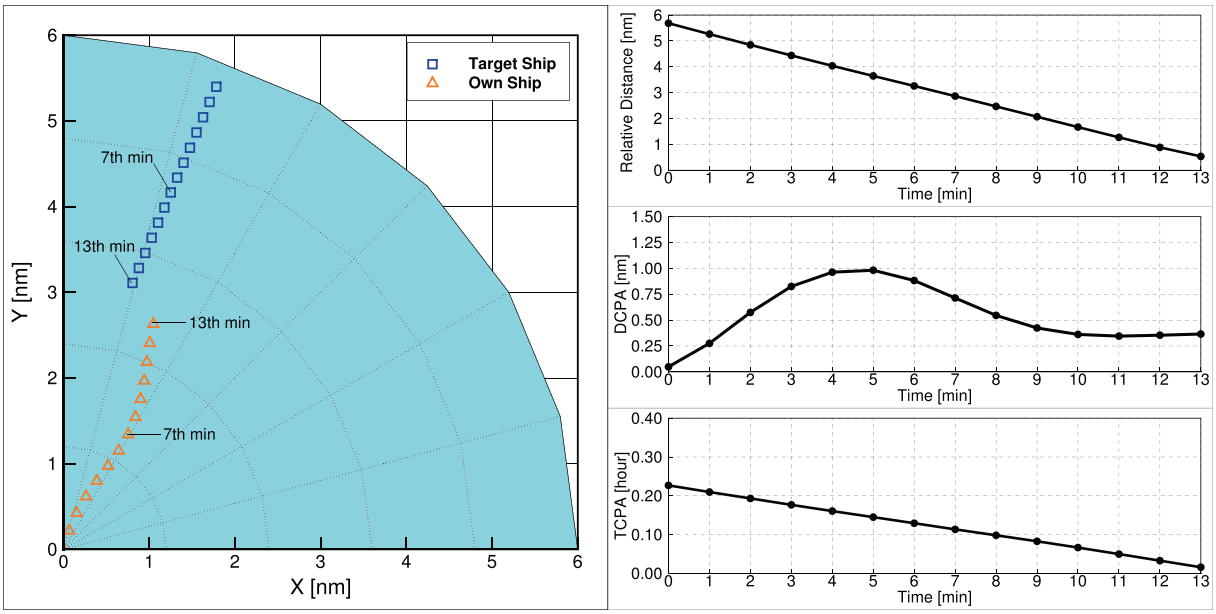

Fig. 10. Trajectories during a crossing encounter and the CPA-assessed variables.

DCPA, and TCPA continue to decrease, while the variation in relative bearing persists. This leads to an overall increase in the 'Very High' level of 'Collision Risk'. The fuzzy-based CRI index shows similar trends to the DBN model, exhibiting a gradual increase in risk from the beginning to the end of the voyage. Both models indicate that the ships remain in proximity, as evidenced by low values of DCPA and TCPA. This suggests that the potential risk of collision persists. One important observation is that between the 0th and 5th minutes, the DCPA increases, and the DBN model reflects this change by showing a rise in the 'Low' level of risk during this time interval. This aligns with the expected outcomes, confirming the consistency of the model's predictions.

To directly evaluate the DBN's robustness to corrupted inputs, errors were deliberately introduced into the latitude and longitude values of the OS at the 7th minute of the same crossing encounter (see Fig. 12). These corrupted values exhibited marked deviations from the expected trajectory. As shown in the top-right and bottom-right panels of Fig. 12, representing the conditions before and after the corruption, the DBN's risk assessment demonstrated notable stability. The probability of the medium-risk level decreased from 68 % to 52 %, yet the 'Medium' level continued to be identified as the most probable outcome. These findings provide evidence of the DBN's resilience to noisy AIS data and its capacity to deliver reliable outputs even under conditions of data corruption.

Another crossing encounter situation is analysed, with the trajectories of the ships and the CPA-assessed variables over time shown in Fig. 13. In this scenario, the TS is positioned on the starboard side of the OS, indicating that the encounter is classified as a crossing situation according to COLREG. As the give-way vessel, the OS is required to take action. In this particular encounter, however, the OS maintained its course, likely due to the sufficient distance between the vessels. The initial relative distance between the ships is 6 nm. Although the DCPA increases slightly, suggesting a reduced potential for collision, both the TCPA and relative distance decrease in parallel, following a consistent trend. As illustrated in Fig. 14, the fuzzy-based CRI shows a steady increase, even as the DCPA rises, which may seem counterintuitive when evaluating the real-world scenario. In contrast, the DBN-based model initially predicts a 'Low'

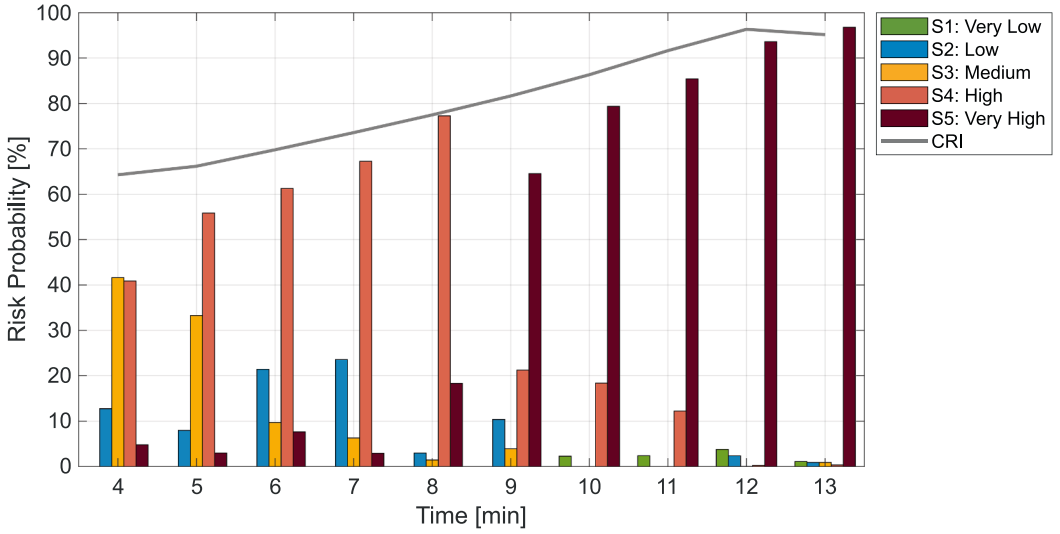

Fig. 11. Collision risk assessment for the OS with respect to the TS in a crossing encounter.

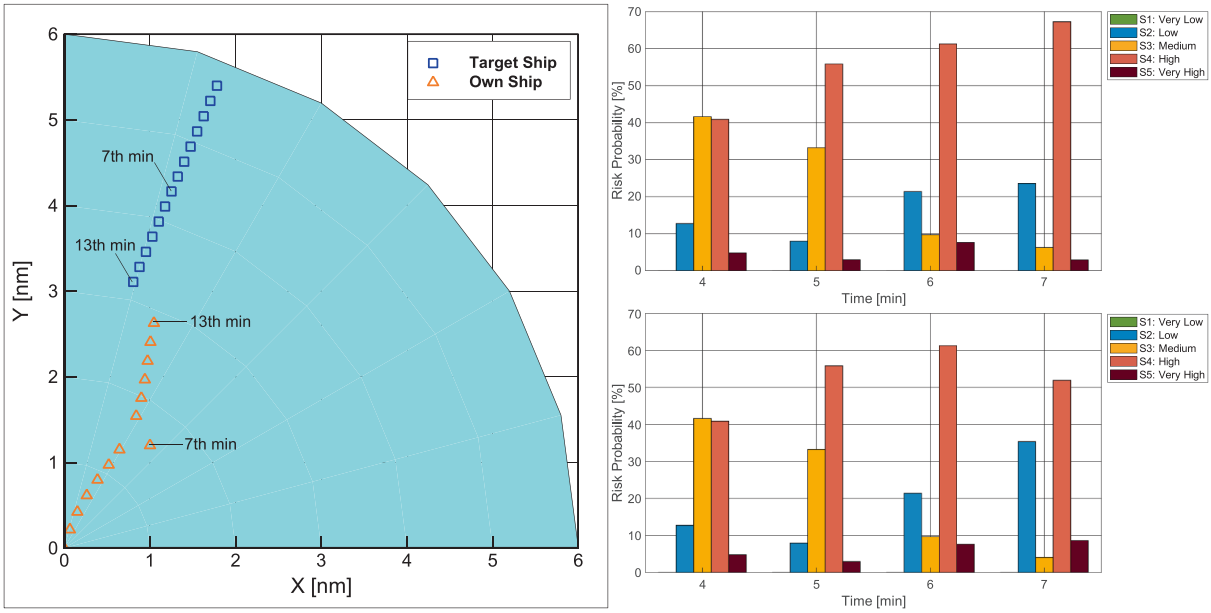

Fig. 12. DBN assessment before and after the introduction of corrupted AIS inputs.

collision risk, which gradually increases to a 'High' risk until the 9th minute. After this point, the increase in DCPA becomes the dominant factor, while both TCPA and relative distance continue to decrease. As a result, the 'High' collision risk begins to subside, and the model outputs a distribution of 'Medium', 'Low', and 'Very Low' risks, with a value of around 30 %. Interestingly, at the 18th minute, when the OS is ahead of the TS, one would generally expect a lower collision risk unless there is a course alteration by either vessel. However, the fuzzy-based model predicts an overestimated risk index at this stage, leading to a misevaluation of the situation.

(2) Head-on encountering.

To further evaluate the performance of the DBN model, another encounter situation is analysed. In Fig. 15, based on the initial positions and courses of the OS and TS, the encounter is classified as a typical head-on situation according to the COLREG. In this scenario, both vessels are required to manoeuvre toward their respective starboard sides. The trajectories in the figure demonstrate that both ships adhered to these rules during the encounter. Throughout the encounter, the fuzzy-based CRI remained between 38 % and 50 %. In contrast, the DBN model initially predicted a 'High' level of collision risk, approaching 100 %. This was largely due to the DCPA being in state S1, which significantly impacts the collision risk. The 'High' risk level persisted for some time before gradually decreasing after the 13th minute, as shown in Fig. 16. After this point, the risk levels shifted to 'Very Low', 'Low', and 'Medium',

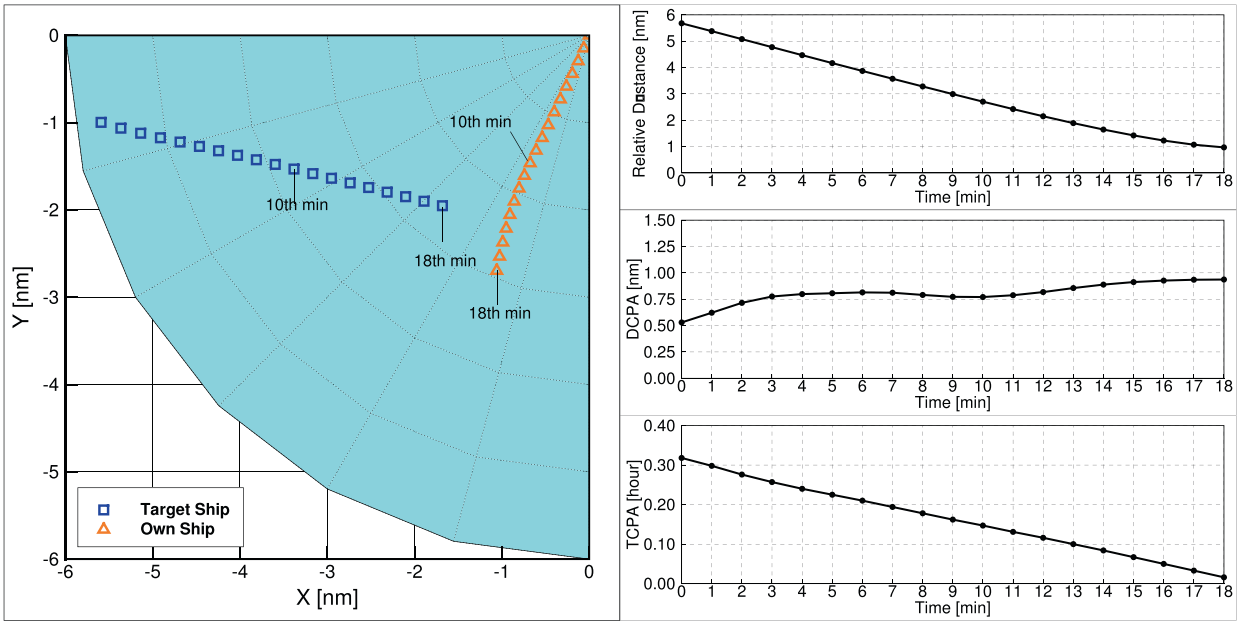

Fig. 13. Trajectories during a crossing encounter and the CPA-assessed variables.

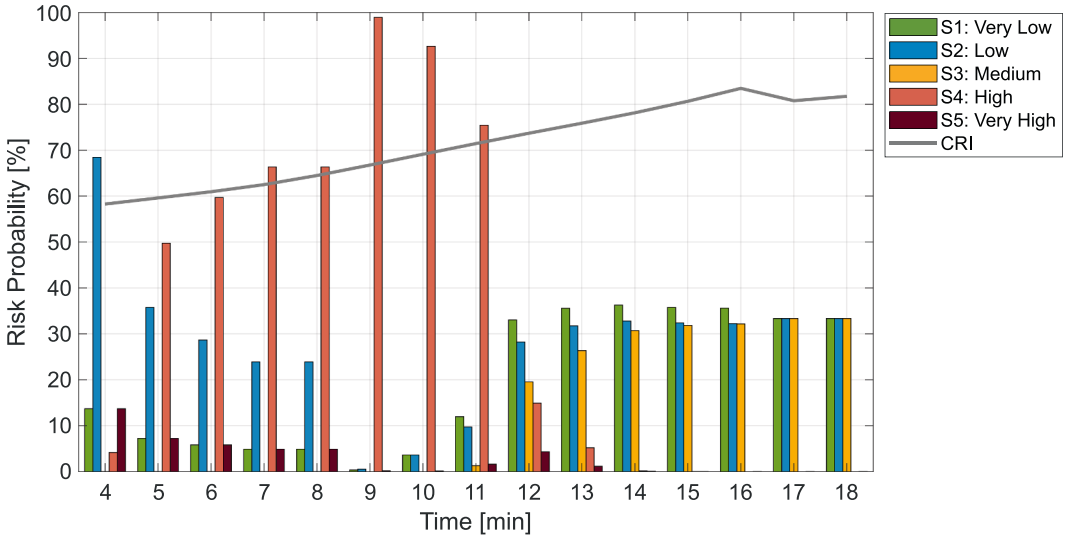

Fig. 14. Collision risk assessment for the OS with respect to the TS in a crossing encounter.

indicating that the potential for collision had significantly reduced.

The DBN model predicted a 'Very High' level of collision risk, peaking at 65 % between the 10th and 13th minutes. This observation was further investigated to understand the underlying dynamics. During this time, the TS executed aggressive manoeuvring toward its starboard side, which amplified the variation in relative bearing. As illustrated in Fig. 17(a), at the 10th minute, the state of relative bearing variation was entirely in state S4 (100 %). Over the following minutes (Figs. 17(b) to 16(d)), the proportion of state S5 gradually increased while the proportion of state S4 decreased. These aggressive manoeuvres were effectively captured by the DBN model, which reflected the increasing probability of the 'Very High' collision risk level in the predictions.

(3) Overtaking encountering.

In Fig. 18, the initial positions of the ships indicate that the OS is being overtaken by the TS. At this stage, the DBN model predicts a 'High' level of collision risk, approaching 100 %, due to the proximity of the vessels. The DCPA remains near zero between the 8th and 14th minutes, suggesting that if both ships maintain their current course and speed, a collision is inevitable, as shown in Fig. 19. During this interval, the DBN model assigns a 'Very High' collision risk level, primarily driven by the minimal DCPA and sudden variation in relative bearing. After the 14th minute, however, the DCPA increases significantly and stabilises between the 17th and 34th minutes.

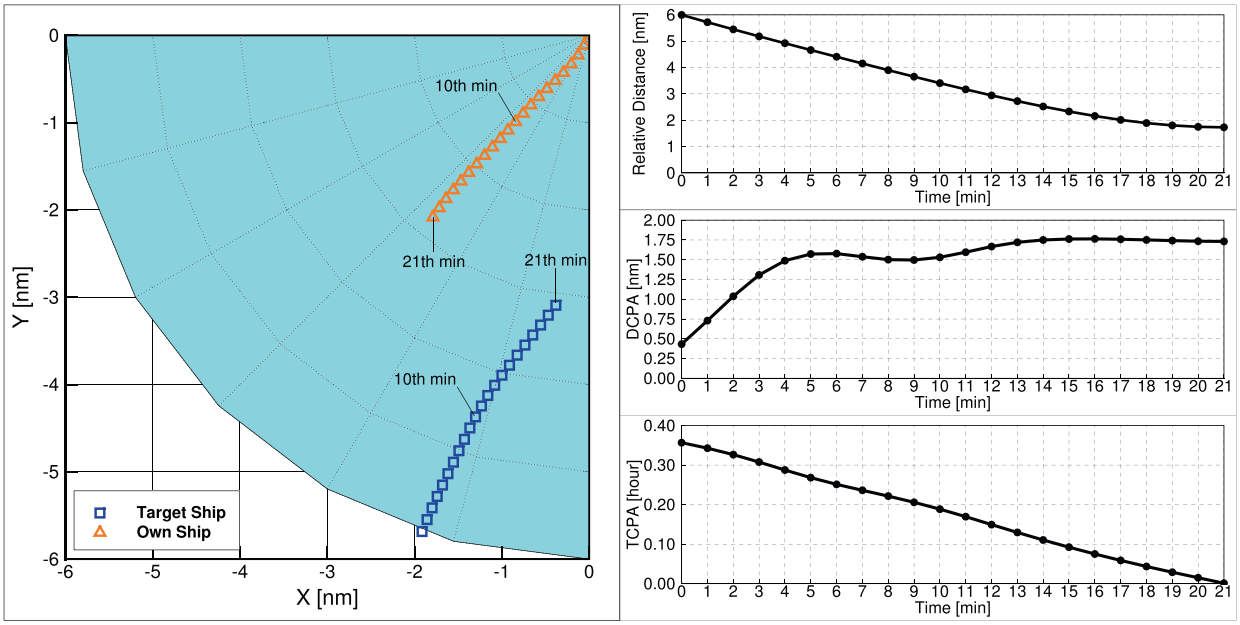

Fig. 15. Trajectories during a head-on encounter and the CPA-assessed variables.

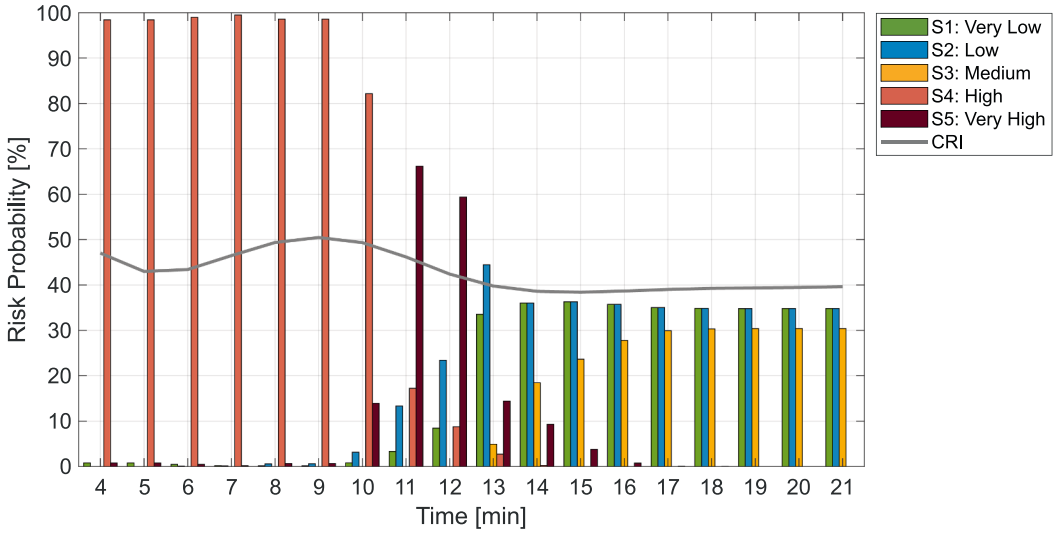

Fig. 16. Collision risk assessment for the OS with respect to the TS in a head-on encounter.

During this period, both the TCPA and the relative distance gradually decrease. Consequently, the DBN model predicts 'Very Low' and 'Low' collision risk levels, with an average probability of around 50 % for both. Notably, after the 27th minute, the model shows a slight increase in the 'Medium' collision risk level. This increase is attributed to the decreasing relative distance and TCPA, indicating a shift in the encounter dynamics.

4.2. Simulation scenario for multi-ship encounters

A simulation scenario is configured to analyse multi-ship encounters. In this setup, the OS is positioned at the origin (0, 0), while the positions of the other ships are determined based on different encounter situations, as shown in Fig. 20. The ships' positions, speeds, and course directions are summarised in Table 7. These parameters are carefully selected to simulate a collision scenario at coordinates (0, 7.5), closely resembling the scenario created by Liu et al. (2024).

The DBN model is then employed to predict the collision risk between the OS and the target ships. Initially, TS1, approaching from the head-on direction, presents the lowest collision risk to the OS, predominantly showing 'Very Low' and 'Low' risk levels, as

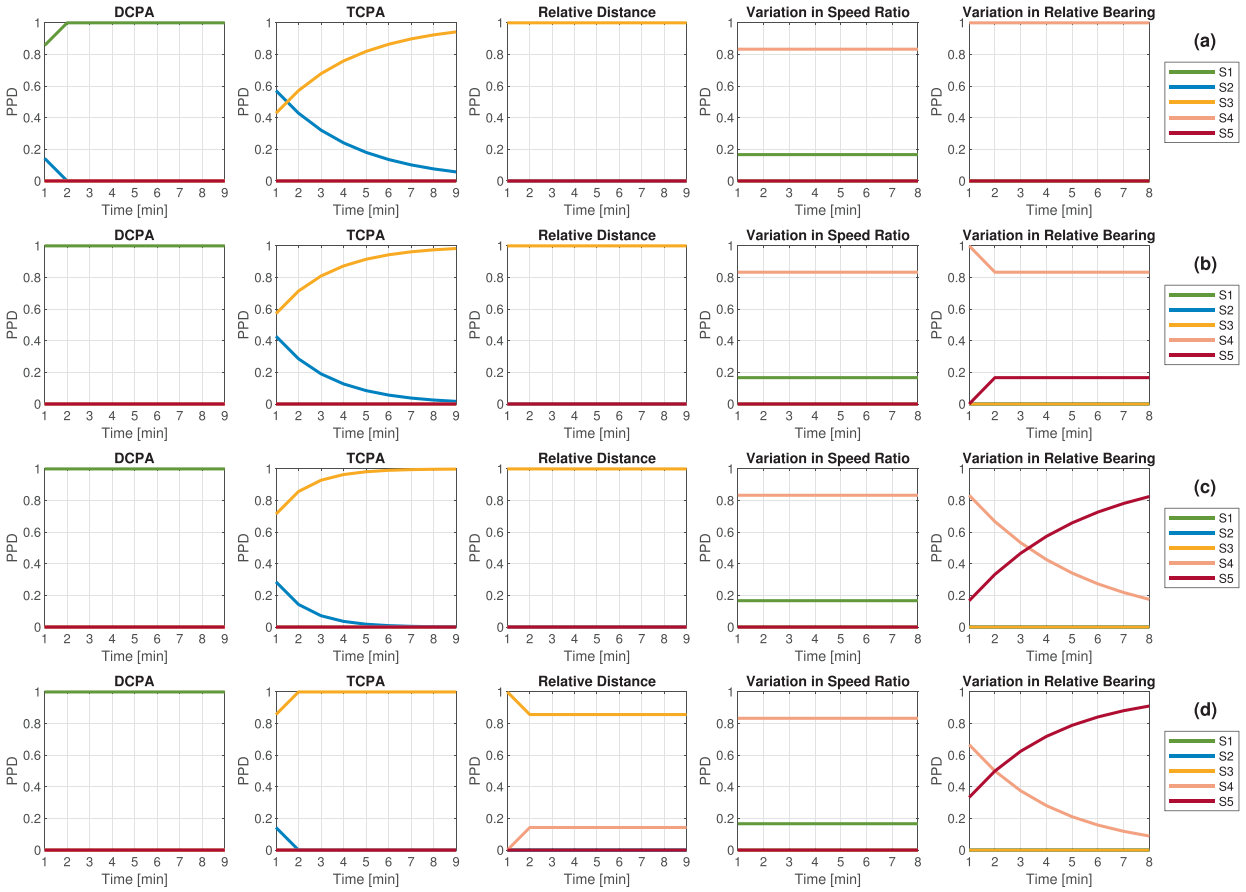

Fig. 17. State transitions of the RIFs at 10th(a), 11th(b), 12th(c), and 13th(d) minutes.

illustrated in Fig. 21. In contrast, TS2, approaching from the crossing direction, poses a higher risk than TS1, with the collision risk classified as 100 % at the 'Medium' level, as shown in Fig. 22. The highest risk in the initial configuration is associated with TS3, where the OS is in an overtaking situation relative to TS3. In this overtaking scenario, the risk levels are classified as 'Medium,' 'High,' and 'Very High,' with respective probabilities of 40 %, 40 %, and 20 %, as seen in Fig. 23.

Over time, TS2 reaches a dominant 'High' level of risk at the 15th minute, before TS1 reaches the same risk level at the 18th minute. Throughout the scenario, TS3 maintains the highest risk level relative to the OS. Additionally, TS2 reaches the 'Very High' risk level at the 22nd minute, while TS1 reaches this level later, at the 25th minute. Notably, the transition in risk levels for TS1 occurs more rapidly than for TS2, due to the higher relative velocity between TS1 and the OS.

The DBN model effectively classifies the collision risks between the OS and the target ships, demonstrating its potential as a robust decision-making tool. It offers valuable insights for prioritising actions to mitigate risks, enabling effective risk management within a sufficient timeframe.

4.3. Discussions

Traditional geometrical-based probability methods, as well as advanced variants, often fail to accurately assess collision risks in certain encounter situations. These methods tend to lack robustness, particularly in identifying the most hazardous TS relative to the OS. One of the major limitations of these approaches is their inability to effectively evaluate continuous collision risk values, especially in head-on and overtaking scenarios. This is primarily because they treat the ship as a single velocity point, failing to capture the kinematic interactions between vessels (Du et al., 2020). Consequently, these models often offer an oversimplified view of the situation, neglecting critical dynamic factors such as variation in speed ratio and relative bearing. To address these limitations, a DBN-based model has been developed that incorporates these novel factors, which are key indicators that emerge from the complex kinematic interactions between ships, allowing for a more accurate and dynamic assessment of collision risk. By embedding these elements, the DBN advances beyond traditional methods by providing continuous, real-time predictions that reflect the evolving nature of encounters.

One of the key challenges in collision risk assessment lies in evaluating evasive manoeuvres. Traditional geometric probability-based methods rely on parameters such as DCPA, TCPA, and relative distance, which, although useful, fail to adequately capture

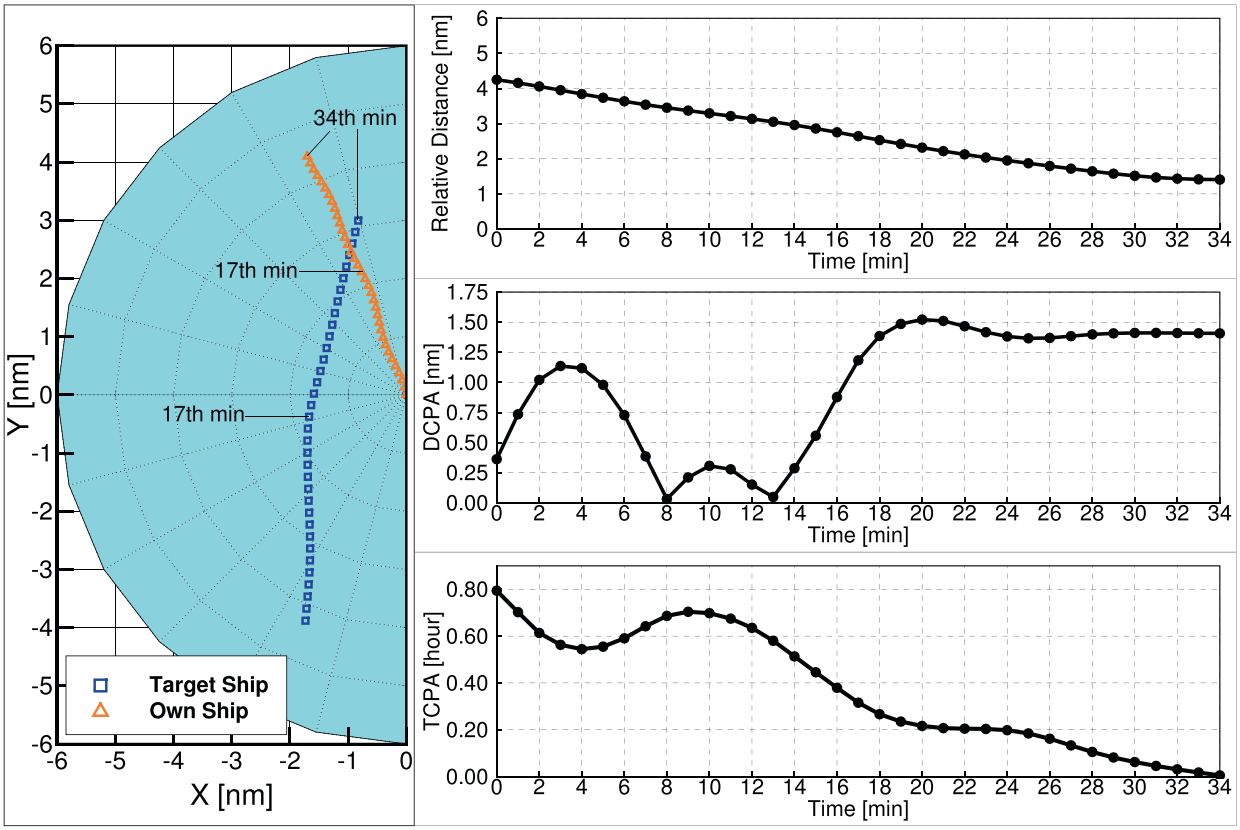

Fig. 18. Trajectories during an overtaken encounter and the CPA-assessed variables.

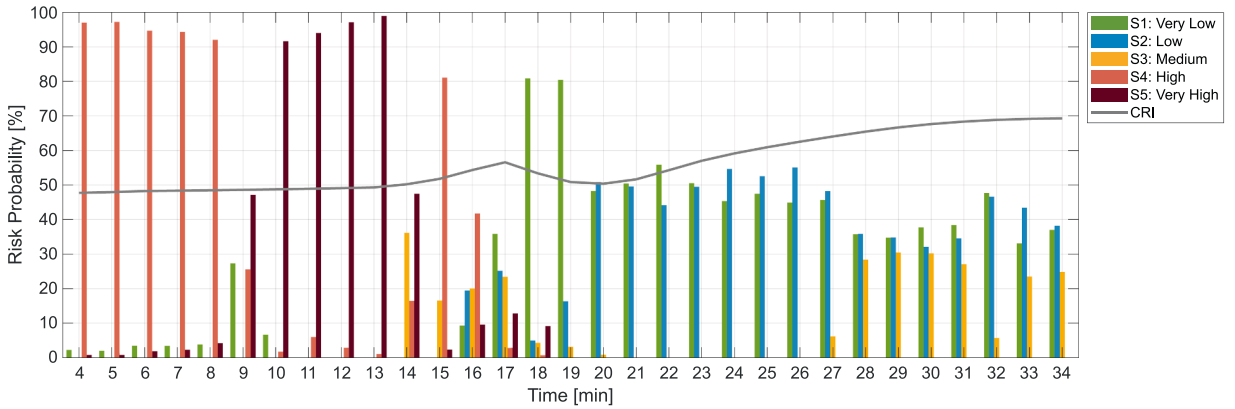

Fig. 19. Collision risk assessment for the OS with respect to the TS in an overtaken encounter.

evasive actions. These methods are limited in their ability to model the temporal and spatial complexity of evasive manoeuvres. In contrast, the DBN model overcomes this limitation by introducing the variation in speed ratio and relative bearing as novel factors, offering a deeper understanding of the vessels' relative motion and enhancing the assessment of collision risk.

In this study, the DBN model is compared with an advanced fuzzy-based CRI model. While the fuzzy-based CRI model provides useful insights, it fails to assess collision risk accurately and consistently in some scenarios. For instance, in certain encounter situations, the fuzzy-based CRI model often predicts a risk index value close to 100 %, even in the absence of genuine collision threats, highlighting the limitations of fuzzy logic in dynamic maritime environments. In contrast, the DBN model demonstrated a superior ability to evaluate potential collision risks by using discrete risk levels, effectively representing varying degrees of danger as the encounter progresses. Its dynamic and evolving assessments offer a more accurate representation of changing encounter dynamics.

In multi-ship encounter scenarios, it is not sufficient to rely solely on distance and time-based parameters to prioritise actions. A

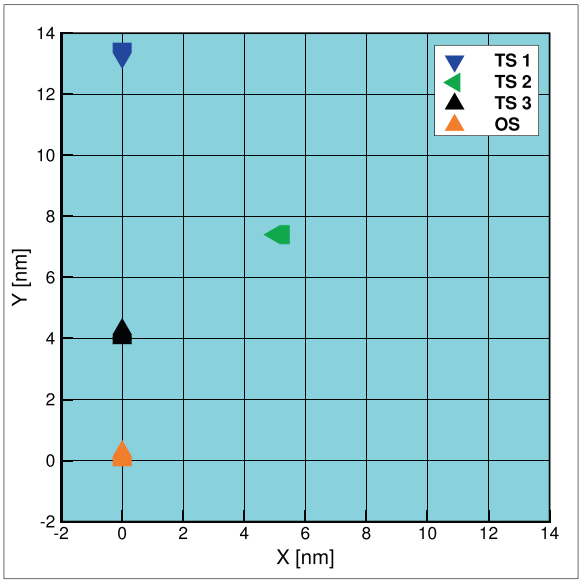

Fig. 20. Initial positions of the OS and TSs in multi-ship encounters.

Table 7
Initial configuration of the multi-ship encounters.

Ship	Position [nm]	Course [deg]	Speed [knot]
OS	(0,0)	0	15
TS1	(0,13.5)	180	12
TS2	(5,7.5)	270	10
TS3	(0,4)	0	7

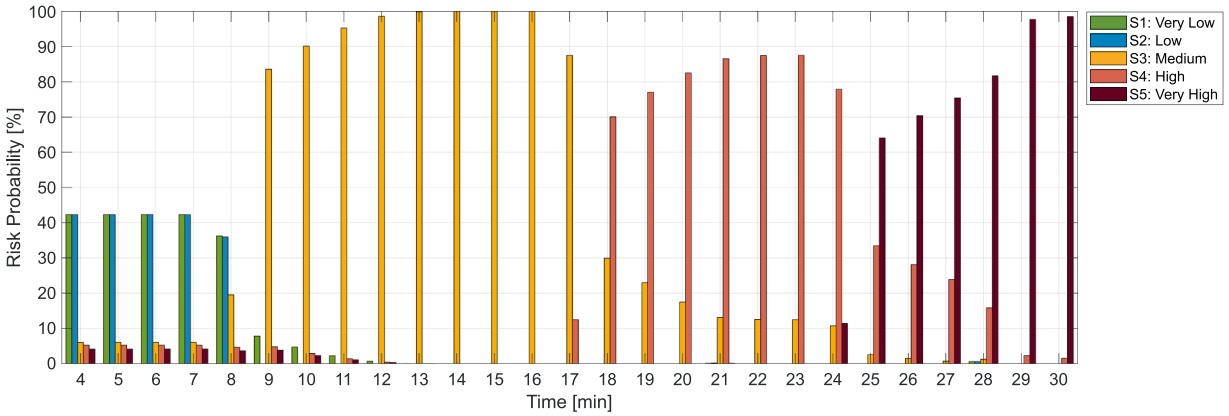

Fig. 21. Collision risk assessment for the OS with respect to the TS1.

broader analysis that integrates multiple variables is necessary to identify which TS poses the greatest collision risk to the OS. The DBN addresses this challenge by providing discrete risk levels through the integration of dynamic factors such as ship behaviour and relative motions. This comprehensive approach enables accurate prioritisation of potential collision risks with respect to the OS and supports more effective collision-avoidance decision-making.

Overall, the DBN model represents a significant advancement in collision risk assessment. By integrating multiple dynamic factors, it provides a more accurate, real-time evaluation of potential collisions, which is crucial for ensuring the safety of maritime operations. Its adaptability to diverse encounter scenarios and continuous adjustment of predictions offer a robust framework for collision risk management, positioning the model as a key component in the development of intelligent decision-support systems for autonomous vessels.

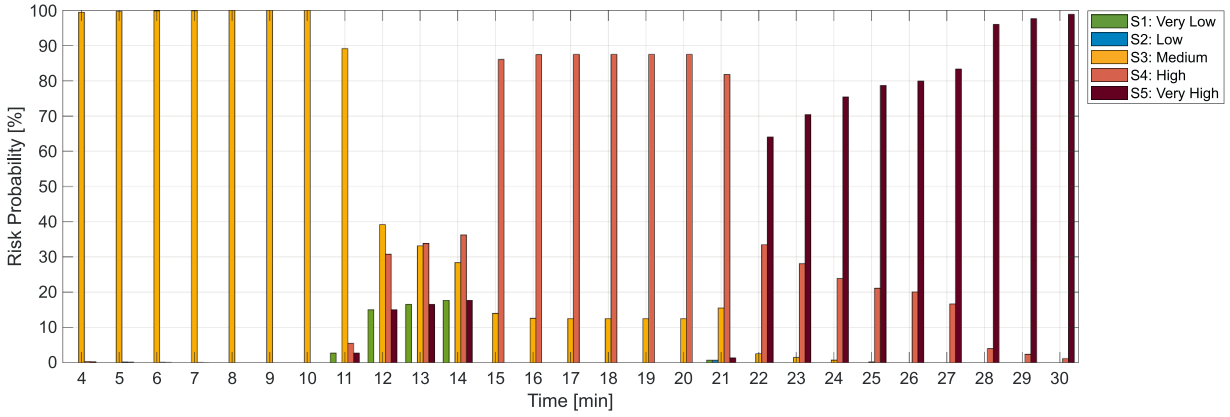

Fig. 22. Collision risk assessment for the OS with respect to the TS2.

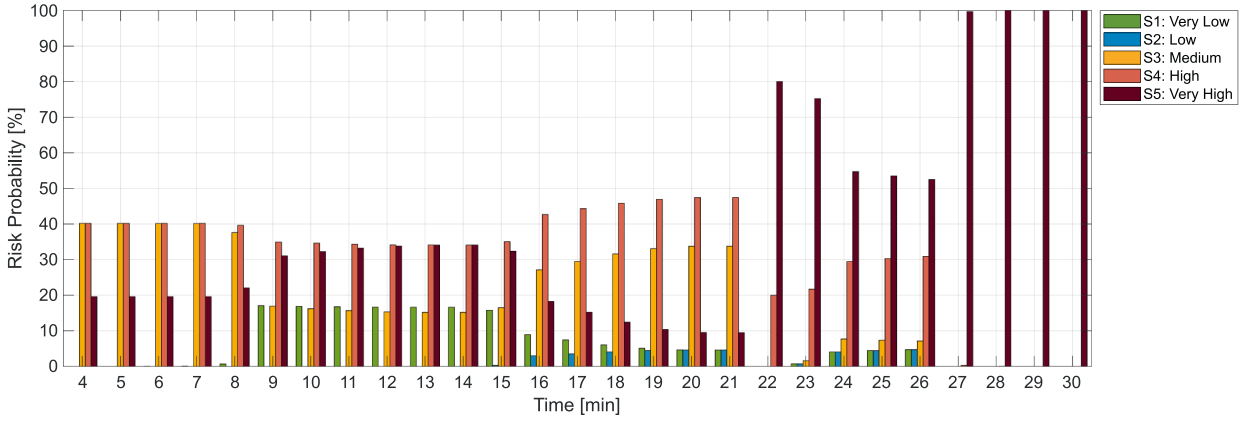

Fig. 23. Collision risk assessment for the OS with respect to the TS3.

5. Applications and implications

The proposed DBN model represents a significant advancement in collision risk prediction for both conventional and autonomous maritime navigation. Its ability to dynamically assess risk levels in real-time while incorporating historical voyage data makes it a valuable tool for diverse stakeholders in the maritime industry. The following implications outline its practical applications and potential impact across various domains.

5.1. Applications for maritime collision risk management

The DBN model significantly enhances predictive accuracy for collision avoidance by incorporating aggressive manoeuvring actions, which are often overlooked in traditional CRI methods. By integrating variation in speed ratio and relative bearing, the model achieves greater precision in identifying high-risk scenarios. This real-time risk assessment capability allows for more informed navigational decisions, reducing the likelihood of accidents, specifically in congested waters.

Another major advantage of the DBN model is its seamless integration with MASS. Although it was developed using data from conventional ships, the RIFs remain applicable to autonomous vessels, making the model a viable candidate for integration into MASS navigation and collision avoidance systems. The proposed DBN model can be integrated into MASS collision-avoidance and decision-support modules by providing real-time probabilistic risk prediction. Depending on the operational setup, these predictions can trigger risk-based decision mechanisms. For instance, predictions exceeding a given threshold may initiate COLREG-compliant encounters evasive manoeuvres (Wang et al., 2024a) or feed into probabilistic optimisation frameworks (Wang et al., 2024b) to determine the most effective evasive actions in complex, multi-ship environments. This ensures that autonomous ships can use historical AIS data to enhance their decision-making capabilities, reducing reliance on human intervention and improving situational awareness in high-traffic maritime zones.

Additionally, the DBN model serves as an effective decision-support tool for maritime safety operations. By categorising collision

risk into five levels, 'Very Low', 'Low', 'Medium', 'High', and 'Very High', it provides actionable insights into the accident likelihood. Simulation results indicate that when the probability of the 'Very High' state exceeds 80 %, collision likelihood becomes critical, offering an early-warning mechanism for preventive action.

The model's capability to process raw AIS data further strengthens its real-world applicability. Unlike traditional risk assessment models that are sensitive to noise in AIS data, the DBN model incorporates historical voyage data to refine predictions. This reduces false alarms, ensures a more reliable risk evaluation, and enhances the accuracy of collision risk assessment in dynamic maritime environments.

5.2. Implications for maritime stakeholders

For port authorities and maritime regulators, the DBN model strengthens compliance with maritime safety regulations, such as the COLREG. By providing real-time risk assessments, authorities can implement risk-based traffic management strategies and enforce navigation restrictions in high-risk maritime zones. This enhances overall navigational safety and ensures proactive collision avoidance measures.

For shipowners and fleet managers, the DBN model offers an advanced tool for real-time risk monitoring and fleet safety management. Integrated into fleet management systems, it allows operators to track risks across multiple vessels, minimising operational disruptions and improving overall fleet safety. Additionally, by reducing accident occurrences, shipowners can lower insurance costs, minimise vessel damage-related expenses, and extend the lifespan of their fleet.

For maritime insurance companies, the DBN model provides a dynamic risk-based approach to insurance premium adjustments. Beyond reliance on historical accident data, insurers can use real-time collision risk assessments to develop tailored maritime insurance policies. The model also strengthens underwriting processes by providing probabilistic analyses of accident likelihood, supporting more precise risk evaluation criteria.

For MASS developers and autonomous navigation systems, the DBN model serves as a critical component for autonomous collision avoidance. Given that it effectively functions without pre-processed AIS data, it is highly adaptable to AI-driven vessel navigation. Moreover, its ability to update risk probabilities in real-time aligns with the needs of next-generation autonomous vessels, ensuring safer and more informed navigation decisions. By continuously updating risk levels based on raw AIS data, the model enables autonomous ships to prioritise evasive actions, optimise route planning, and improve situational awareness in congested maritime environments.

For maritime researchers and AI developers, the DBN model provides a valuable foundation for further advancements in AI-driven collision risk modelling. Researchers can expand upon this model by incorporating additional influencing factors, refining machine learning-based prediction techniques, and integrating multi-sensor data fusion methods. This enables further innovations in maritime safety and risk assessment technologies.

The DBN-based collision risk prediction model marks a major advancement in maritime safety, delivering real-time, data-driven insights into collision risks for both conventional and autonomous ships. Its ability to process raw AIS data, account for aggressive manoeuvring actions, and categorise risk levels enhances its practical applicability across various stakeholders. By integrating this model into maritime operations, policy-making, and autonomous systems, the industry can significantly reduce collision risks, enhance navigational safety, and pave the way for the next generation of autonomous shipping technologies.

6. Conclusions

This study presents a DBN-based collision risk prediction methodology that integrates deterministic geometric models with probabilistic causation-based approaches. While it utilises functional parameters similar to conventional models, this study represents the first application of DBN in ship-to-ship collision risk analysis using raw AIS data. Unlike existing models, which rely solely on predefined risk indicators, the proposed DBN model incorporates additional parameters, such as variation in speed ratio and relative bearing, which play a crucial role in detecting aggressive or evasive manoeuvres that may escalate collision risks. This comprehensive approach significantly improves the interpretability and predictive accuracy of collision risk assessments. A major contribution of this study is the integration of mutual relationships among influencing factors, rather than treating them as independent variables. This allows for a more realistic and dynamic assessment of risk, providing five discrete risk levels ranging from 'Very Low' to 'Very High', offering an intuitive representation of potential collision threats. Real-world case studies and simulation results further validate the superiority of the DBN model over traditional methods, such as fuzzy-based CRI models. Notably, in low-risk scenarios, the DBN model correctly reflected expected outcomes, whereas CRI models produced misleading results. Additionally, when the collision risk exceeds the 'Very High' level of 80 %, a collision is highly probable within a short timeframe unless immediate avoidance actions are taken.

Beyond its enhanced predictive capabilities, the DBN model is highly adaptable, making it particularly suitable for application in MASS and autonomous navigation systems. In multi-ship encounter scenarios, it effectively prioritises risk among multiple surrounding vessels, providing an enhanced situational awareness framework for autonomous decision-making systems. Moreover, its ability to process raw AIS data in real-time ensures that navigational adjustments can be made proactively, reducing collision risks in congested maritime environments. In summary, the DBN-based collision risk assessment model offers a robust, data-driven approach that outperforms conventional methods by incorporating probabilistic reasoning, mutual influence relationships, and real-time adaptability. Given its ability to process real-time AIS data and adaptively update collision risk, the proposed framework can serve as a robust decision-support tool for autonomous navigation systems, supporting the safe deployment of MASS in mixed traffic conditions. This advancement holds significant promise for enhancing maritime safety, particularly in the transition toward fully

autonomous navigation systems.

Future research should focus on optimising the model, incorporating multi-sensor data fusion, and extending its application to broader maritime risk management frameworks, such as grounding risks, extreme weather hazards, and port congestion analysis. Additionally, future research should focus on deploying the model in real-world autonomous ship trials to validate its effectiveness under fully automated navigation scenarios.

CRediT authorship contribution statement

Cihad Çelik: Writing – review & editing, Writing – original draft, Visualization, Validation, Software, Resources, Methodology, Investigation, Formal analysis, Data curation, Conceptualization. **Huanhuan Li:** Writing – review & editing, Writing – original draft, Visualization, Validation, Supervision, Project administration, Methodology, Formal analysis, Conceptualization. **Jiongjiong Liu:** Writing – review & editing, Visualization, Investigation, Data curation. **Musa Bashir:** Writing – review & editing, Validation, Supervision, Formal analysis. **Lu Zou:** Writing – review & editing, Visualization, Validation, Supervision. **Zaili Yang:** Writing – review & editing, Visualization, Supervision, Resources, Methodology, Funding acquisition, Formal analysis.

Declaration of competing interest

The authors declare that they have no known competing financial interests or personal relationships that could have appeared to influence the work reported in this paper.

Acknowledgement

This project has received funding from the European Research Council (ERC) under the European Union's Horizon 2020 research and innovation programme (Grant Agreement No. 864724).

Appendix A

Variables in membership functions

$$d_1 = \begin{cases} 1.1 - 0.2\theta_T/180^\circ & 0 \le \theta_T < 112.5^\circ \\ 1.0 - 0.4\theta_T/180^\circ & 112.5^\circ \le \theta_T < 180^\circ \\ 1.0 - 0.4(360^\circ - \theta_T)/180^\circ & 180^\circ \le \theta_T < 247.5^\circ \\ 1.1 - 0.2(360^\circ - \theta_T)/180^\circ & 247.5^\circ \le \theta_T < 360^\circ \end{cases} \tag{A-1}$$

$$d_2 = 2d_1 \tag{A-2}$$

$$t_1 = \begin{cases} \dfrac{\sqrt{D_1^2 - DCPA^2}}{V_R} & |DCPA| \le D_1 \\ \dfrac{D_1 - |DCPA|}{V_R} \end{cases}$$

$$|DCPA| > D_1 \tag{A-3}$$

$$t_2 = \frac{\sqrt{12^2 - DCPA^2}}{V_R} \tag{A-4}$$

$$D_1 = (8-12)L \tag{A-5}$$

$$D_2 = 1.7cos(\theta_T - 19^\circ) + \sqrt{4.4 + c2.89os^2(\theta_T - 19^\circ)} \tag{A-6}$$

$$C = \cos^{-1}\left(\frac{V_{OX}V_{TX} + V_{OY}V_{TY}}{\sqrt{(V_{OX}^2 + V_{OY}^2)(V_{TX}^2 + V_{TY}^2)}}\right) \tag{A-7}$$

Appendix B

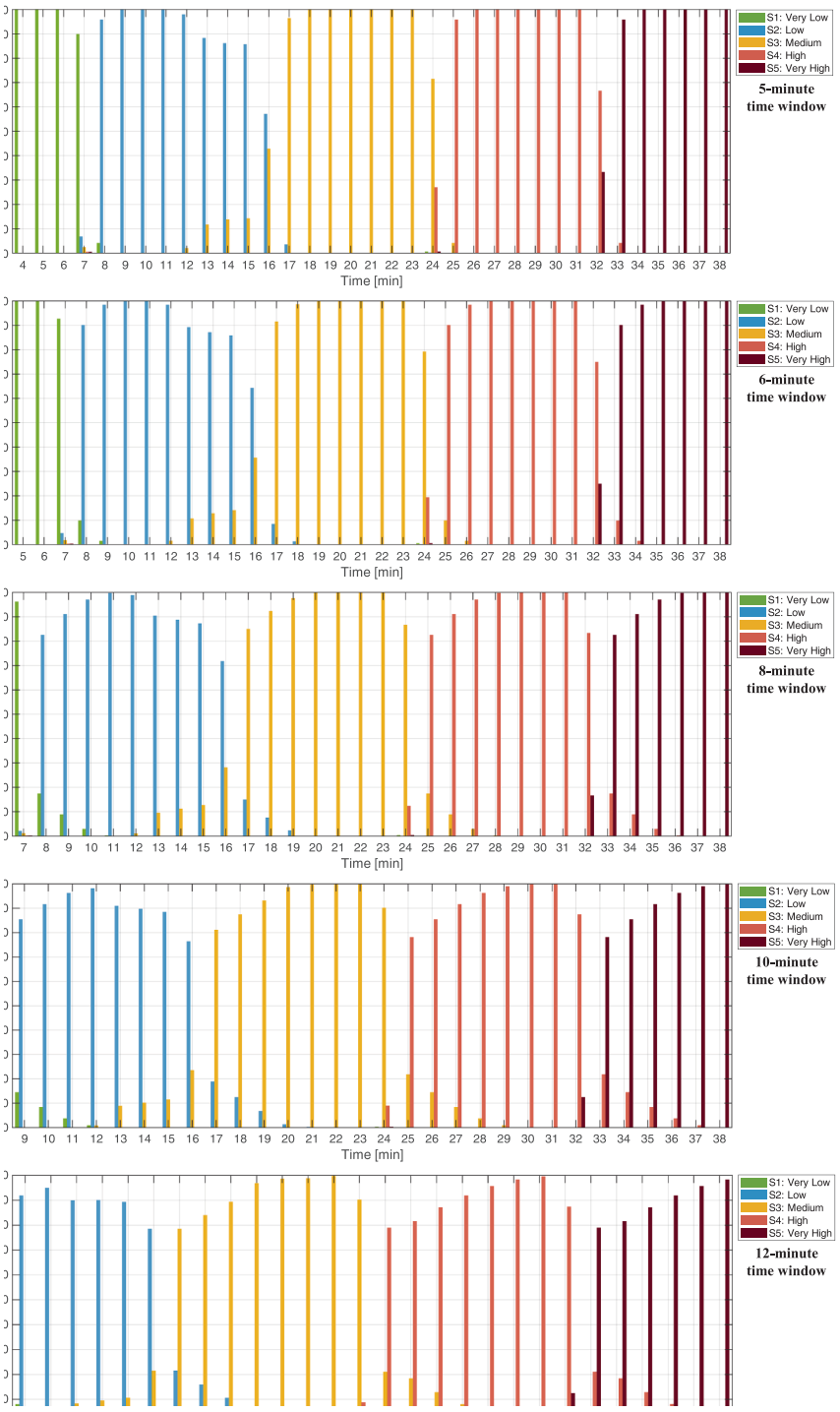

Fig. B1. Effect of varying time windows (5, 6, 8, 10, and 12 min) on the predicted collision risk levels for the CF CRYSTAL – SANCHI encounter.

Data availability

The authors do not have permission to share data.

References

Abebe, M., Noh, Y., Seo, C., Kim, D., Lee, I., 2021. Developing a Ship Collision Risk Index estimation model based on Dempster-Shafer theory. Appl. Ocean Res. 113, 102735. https://doi.org/10.1016/j.apor.2021.102735.

Antão, P., Sun, S., Teixeira, A.P., Soares, C.G., 2023. Quantitative assessment of ship collision risk influencing factors from worldwide accident and fleet data. Reliab. Eng. Syst. Saf. 234, 109166.

Chen, P., Huang, Y., Mou, J., van Gelder, P.H.A.J.M., 2019a. Probabilistic risk analysis for ship-ship collision: State-of-the-art. Saf. Sci. 117, 108–122. https://doi.org/10.1016/j.ssci.2019.04.014.

Chen, P., Huang, Y., Mou, J., van Gelder, P.H.A.J.M., 2018. Ship collision candidate detection method: a velocity obstacle approach. Ocean Eng. 170, 186–198. https://doi.org/10.1016/j.oceaneng.2018.10.023.

Chen, P., Mou, J., van Gelder, P.H.A.J.M., 2019b. Integration of individual encounter information into causation probability modelling of ship collision accidents. Saf. Sci. 120, 636–651. https://doi.org/10.1016/j.ssci.2019.08.008.

Coldwell, T.G., 1983. Marine Traffic Behaviour in Restricted Waters. J. Navig. 36, 430–444. https://doi.org/10.1017/S0373463300039783.

Cui, Z., Guan, W., Zhang, X., 2025. Gated transformer-based proximal policy optimization for multiple marine autonomous surface ships collision avoidance decision-making strategy. Eng. Appl. Artif. Intel. 156, 111242. https://doi.org/10.1016/j.engappai.2025.111242.

Ding, H., Weng, J., Shi, K., 2024. Real-time assessment of ship collision risk using image processing techniques. Appl. Ocean Res. 153, 104241. https://doi.org/10.1016/j.apor.2024.104241.

Du, L., Goerlandt, F., Valdez Banda, O.A., Huang, Y., Wen, Y., Kujala, P., 2020. Improving stand-on ship's situational awareness by estimating the intention of the give-way ship. Ocean Eng. 201, 107110. https://doi.org/10.1016/j.oceaneng.2020.107110.

Fan, H., Jia, H., He, X., Lyu, J., 2024a. Navigating uncertainty: a dynamic Bayesian network-based risk assessment framework for maritime trade routes. Reliab. Eng. Syst. Saf. 250, 110311. https://doi.org/10.1016/j.ress.2024.110311.

Fan, L., Zhao, Z., Yin, J., 2024b. Research on dynamic influence mechanism of port state control and ship risk level. Ocean Coast. Manag. 250, 107028. https://doi.org/10.1016/j.ocecoaman.2024.107028.

Fujii, Y., Tanaka, K., 1971. Traffic Capacity. J. Navig. 24, 543–552. https://doi.org/10.1017/S0373463300022384.

Goerlandt, F., Montewka, J., Kuzmin, V., Kujala, P., 2015. A risk-informed ship collision alert system: Framework and application. Saf. Sci. 77. https://doi.org/10.1016/j.ssci.2015.03.015.

Goodwin, E.M., 1975. A Statistical Study of Ship Domains. J. Navig. 28, 328–344. https://doi.org/10.1017/S0373463300041230.

Guo, W., Zhang, X., Ge, Y.-E., Du, Y., 2025a. Deep Q-network and knowledge jointly-driven ship operational efficiency optimization in a seaport. Transp. Res. Part E Logist. Transp. Rev. 197, 104046. https://doi.org/10.1016/j.tre.2025.104046.

Guo, W., Zhang, X., Li, Y., Zhang, L., 2025b. Collaborative optimization of vessel scheduling and tugboat allocation in seaports using a multi-action deep reinforcement learning framework. Eng. Appl. Artif. Intel. 156, 111239. https://doi.org/10.1016/j.engappai.2025.111239.

Guo, Y., Jin, Y., Hu, S., Yang, Z., Xi, Y., Han, B., 2023. Risk evolution analysis of ship pilotage operation by an integrated model of FRAM and DBN. Reliab. Eng. Syst. Saf. 229, 108850. https://doi.org/10.1016/j.ress.2022.108850.

Halliday, J., Gayle, D., 2025. North Sea collision: foul play, technical fault or human error? The Guardian.

Han, Z., Zhang, D., Fan, L., Zhang, J., Zhang, M., 2024. A Dynamic Bayesian Network model to evaluate the availability of machinery systems in Maritime Autonomous Surface Ships. Accid. Anal. Prev. 194, 107342. https://doi.org/10.1016/j.aap.2023.107342.

He, Z., Liu, C., Chu, X., Wu, W., Zheng, M., Zhang, D., 2024. Dynamic domain-based collision avoidance system for autonomous ships: real experiments in coastal waters. Expert Syst. Appl. 255, 124805. https://doi.org/10.1016/j.eswa.2024.124805.

Hu, X., Xia, H., Xuan, S., Hu, S., 2023. Exploring the Pirate Attack Process Risk along the Maritime Silk Road via Dynamic Bayesian Network Analysis. J. Mar. Sci. Eng. 11, 1430. https://doi.org/10.3390/jmse11071430.

Hu, Y., Zhang, A., Tian, W., Zhang, J., Hou, Z., 2020. Multi-ship collision avoidance decision-making based on collision risk index. J. Mar. Sci. Eng. 8, 640.

Huang, Y., Chen, L., van Gelder, P.H.A.J.M., 2019. Generalized velocity obstacle algorithm for preventing ship collisions at sea. Ocean Eng. 173, 142–156. https://doi.org/10.1016/j.oceaneng.2018.12.053.

Huang, Y., van Gelder, P.H.A.J.M., Wen, Y., 2018. Velocity obstacle algorithms for collision prevention at sea. Ocean Eng. 151, 308–321. https://doi.org/10.1016/j.oceaneng.2018.01.001.

IMO, C., 1972. Convention on the international regulations for preventing collisions at sea. Equasis World Merch, Fleet, p. 2015.

Jiang, Z., Zhang, L., Li, W., 2024. A machine vision method for the evaluation of ship-to-ship collision risk. Heliyon 10. https://doi.org/10.1016/j.heliyon.2024.e25105.

Li, B., Pang, F.-W., 2013. An approach of vessel collision risk assessment based on the D–S evidence theory. Ocean Eng. 74, 16–21. https://doi.org/10.1016/j.oceaneng.2013.09.016.

Li, H., Çelik, C., Bashir, M., Zou, L., Yang, Z., 2024a. Incorporation of a global perspective into data-driven analysis of maritime collision accident risk. Reliab. Eng. Syst. Saf. 249, 110187. https://doi.org/10.1016/j.ress.2024.110187.

Li, H., Jiao, H., Yang, Z., 2023a. AIS data-driven ship trajectory prediction modelling and analysis based on machine learning and deep learning methods. Transp. Res. Part E Logist. Transp. Rev. 175, 103152. https://doi.org/10.1016/j.tre.2023.103152.

Li, H., Ren, X., Yang, Z., 2023b. Data-driven Bayesian network for risk analysis of global maritime accidents. Reliab. Eng. Syst. Saf. 230, 108938.

Li, H., Xing, W., Jiao, H., Yang, Z., Li, Y., 2024b. Deep bi-directional information-empowered ship trajectory prediction for maritime autonomous surface ships. Transp. Res. Part E Logist. Transp. Rev. 181, 103367. https://doi.org/10.1016/j.tre.2023.103367.

Li, M., Mou, J., Chen, P., Rong, H., Chen, L., van Gelder, P.H.A.J.M., 2022a. Towards real-time ship collision risk analysis: an improved R-TCR model considering target ship motion uncertainty. Reliab. Eng. Syst. Saf. 226, 108650. https://doi.org/10.1016/j.ress.2022.108650.

Li, M., Zhang, R., Chen, X., Liu, K., 2022b. Assessment of underwater navigation safety based on dynamic Bayesian network facing uncertain knowledge and various information. Front. Mar. Sci. 9. https://doi.org/10.3389/fmars.2022.1069841.

Li, W., Zhong, L., Liu, Y., Shi, G., 2023c. Ship Intrusion Collision Risk Model based on a Dynamic Elliptical Domain. J. Mar. Sci. Eng. 11, 1122. https://doi.org/10.3390/jmse11061122.

Li, W., Zhong, L., Xu, Y., Shi, G., 2022c. Collision Risk Index Calculation based on an improved Ship Domain Model. J. Mar. Sci. Eng. 10, 2016. https://doi.org/10.3390/jmse10122016.

Li, Z., Hu, S., Zhu, X., Gao, G., Yao, C., Han, B., 2022d. Using DBN and evidence-based reasoning to develop a risk performance model to interfere ship navigation process safety in Arctic waters. Process Saf. Environ. Prot. 162, 357–372. https://doi.org/10.1016/j.psep.2022.03.089.

Liu, J., Zhang, J., Yang, Z., Wan, C., Zhang, M., 2024a. A novel data-driven method of ship collision risk evolution evaluation during real encounter situations. Reliab. Eng. Syst. Saf. 249, 110228. https://doi.org/10.1016/j.ress.2024.110228.

Liu, X., Yuen, K.F., 2025. A systematic review on artificial intelligence applications in seaports – a network analysis approach. Expert Syst. Appl. 289, 128309. https://doi.org/10.1016/j.eswa.2025.128309.

Liu, Y., Xue, Y., Lu, Y., Yuan, L., Li, F., Li, R., 2024b. A Dynamic Bayesian Network model for ship navigation risk in the Arctic Northeast Passage. Ocean Eng. 312, 119024. https://doi.org/10.1016/j.oceaneng.2024.119024.

Liu, Z., Han, Z., Chen, Q., Shi, X., Ma, Q., Cai, B., Liu, Y., 2023a. Risk assessment of marine oil spills using dynamic Bayesian network analyses. Environ. Pollut. 317, 120716. https://doi.org/10.1016/j.envpol.2022.120716.
Liu, Z., Zhang, B., Zhang, M., Wang, H., Fu, X., 2023b. A quantitative method for the analysis of ship collision risk using AIS data. Ocean Eng. 272, 113906. https://doi.org/10.1016/j.oceaneng.2023.113906.
Ma, X., Lan, H., Qiao, W., Han, B., He, H., 2024. On the causation correlation of maritime accidents based on data mining techniques. Proc. Inst. Mech. Eng. Part O J. Risk Reliab. 238, 905–919. https://doi.org/10.1177/1748006X221131717.
Pereira, M.I., Pinto, A.M., 2024. Reinforcement learning based robot navigation using illegal actions for autonomous docking of surface vehicles in unknown environments. Eng. Appl. Artif. Intel. 133, 108506. https://doi.org/10.1016/j.engappai.2024.108506.
Pietrzykowski, Z., Uriasz, J., 2009. The Ship Domain – a Criterion of Navigational Safety Assessment in an Open Sea Area. J. Navig. 62, 93–108. https://doi.org/10.1017/S0373463308005018.
Qiao, Z., Zhang, Y., Wang, S., 2021. A Collision Risk Identification Method for Autonomous Ships based on Field Theory. IEEE Access 9, 30539–30550. https://doi.org/10.1109/ACCESS.2021.3059248.
Rong, H., Teixeira, A.P., Guedes Soares, C., 2022. Ship collision avoidance behaviour recognition and analysis based on AIS data. Ocean Eng. 245, 110479. https://doi.org/10.1016/j.oceaneng.2021.110479.
Rong, H., Teixeira, A.P., Guedes Soares, C., 2021. Spatial correlation analysis of near ship collision hotspots with local maritime traffic characteristics. Reliab. Eng. Syst. Saf. 209, 107463. https://doi.org/10.1016/j.ress.2021.107463.
Rothmund, S.V., Tengesdal, T., Brekke, E.F., Johansen, T.A., 2022. Intention modeling and inference for autonomous collision avoidance at sea. Ocean Eng. 266, 113080. https://doi.org/10.1016/j.oceaneng.2022.113080.
Seo, C., Noh, Y., Abebe, M., Kang, Y.-J., Park, S., Kwon, C., 2023. Ship collision avoidance route planning using CRI-based A* algorithm. Int. J. Nav. Archit. Ocean Eng. 15, 100551.
Shi, J., Liu, Z., Feng, Y., Wang, X., Zhu, H., Yang, Z., Wang, J., Wang, H., 2024. Evolutionary model and risk analysis of ship collision accidents based on complex networks and DEMATEL. Ocean Eng. 305, 117965. https://doi.org/10.1016/j.oceaneng.2024.117965.
Silveira, P. a. M., Teixeira, A.P., Soares, C.G., 2013. Use of AIS Data to Characterise Marine Traffic Patterns and Ship Collision Risk off the Coast of Portugal. J. Navig. 66, 879–898. DOi: 10.1017/S0373463313000519.
Silveira, P., Teixeira, A.P., Guedes Soares, C., 2022. A method to extract the Quaternion Ship Domain parameters from AIS data. Ocean Eng. 257, 111568. https://doi.org/10.1016/j.oceaneng.2022.111568.
Ugurlu, H., Cicek, I., 2022. Analysis and assessment of ship collision accidents using Fault tree and Multiple Correspondence Analysis. Ocean Eng. 245, 110514. https://doi.org/10.1016/j.oceaneng.2021.110514.
Wang, C., Zhang, X., Gao, H., Bashir, M., Li, H., Yang, Z., 2024a. COLERGs-constrained safe reinforcement learning for realising MASS's risk-informed collision avoidance decision making. Knowl.-Based Syst. 300, 112205. https://doi.org/10.1016/j.knosys.2024.112205.
Wang, C., Zhang, X., Gao, H., Bashir, M., Li, H., Yang, Z., 2024b. Optimizing anti-collision strategy for MASS: a safe reinforcement learning approach to improve maritime traffic safety. Ocean Coast. Manag. 253, 107161. https://doi.org/10.1016/j.ocecoaman.2024.107161.
Wang, N., 2010. An Intelligent Spatial Collision Risk based on the Quaternion Ship Domain. J. Navig. 63, 733–749. https://doi.org/10.1017/S0373463310000202.
Wang, Y., Li, P., Hong, C., Yang, Z., 2025. Causation analysis of ship collisions using a TM-FRAM model. Reliab. Eng. Syst. Saf. 260, 111035. https://doi.org/10.1016/j.ress.2025.111035.
Xin, X., Liu, K., Loughney, S., Wang, J., Li, H., Ekere, N., Yang, Z., 2023. Multi-scale collision risk estimation for maritime traffic in complex port waters. Reliab. Eng. Syst. Saf. 240, 109554. https://doi.org/10.1016/j.ress.2023.109554.
Xu, L., Shen, Y., Chen, J., Xiao, G., Liu, L., 2024. Assessing the impact of the Covid-19 epidemic on the resilience of chinese coastal ports. J. Sea Res. 202, 102554. https://doi.org/10.1016/j.seares.2024.102554.
Yao, Y., Yang, Y., Shang, Q., Chen, Y., 2024. Research on Fault Diagnosis of Marine Diesel Engine based on DA-DBN. In: In: 2024 International Conference on Energy and Electrical Engineering (EEE). Presented at the 2024 International Conference on Energy and Electrical Engineering (EEE), pp. 1–6. https://doi.org/10.1109/EEE59956.2024.10709392.
Yoo, Y., Lee, J.-S., 2019. Evaluation of ship collision risk assessments using environmental stress and collision risk models. Ocean Eng. 191, 106527. https://doi.org/10.1016/j.oceaneng.2019.106527.
Yu, Q., Liu, K., Yang, Z., Wang, H., Yang, Z., 2021. Geometrical risk evaluation of the collisions between ships and offshore installations using rule-based Bayesian reasoning. Reliab. Eng. Syst. Saf. 210, 107474.
Yuan, X., Zhang, D., Zhang, J., Zhang, M., Guedes Soares, C., 2021. A novel real-time collision risk awareness method based on velocity obstacle considering uncertainties in ship dynamics. Ocean Eng. 220, 108436. https://doi.org/10.1016/j.oceaneng.2020.108436.
Zeng, M., Wei, Y., Yu, K., Huang, H., Xie, T., 2024. Scenario Deduction of Oil spill from Tankersin a Ship-Ship Collision based on the KnowledgeElement and Dynamic Bayesian Network. Pol. J. Environ. Stud. 33, 4421–4434. https://doi.org/10.15244/pjoes/177436.
Zhang, D., Yan, X.P., Yang, Z.L., Wall, A., Wang, J., 2013. Incorporation of formal safety assessment and Bayesian network in navigational risk estimation of the Yangtze River. Reliab. Eng. Syst. Saf. https://doi.org/10.1016/j.ress.2013.04.006.
Zhang, M., Montewka, J., Manderbacka, T., Kujala, P., Hirdaris, S., 2021. A big Data Analytics Method for the Evaluation of Ship - Ship Collision Risk reflecting Hydrometeorological Conditions. Reliab. Eng. Syst. Saf. 213, 107674. https://doi.org/10.1016/j.ress.2021.107674.
Zhao, L., Fu, X., 2021. A novel index for real-time ship collision risk assessment based on velocity obstacle considering dimension data from AIS. Ocean Eng. 240, 109913. https://doi.org/10.1016/j.oceaneng.2021.109913.
Zhao, Y., Li, W., Shi, P., 2016. A real-time collision avoidance learning system for Unmanned Surface Vessels. Neurocomputing 182, 255–266.
Zhen, R., Riveiro, M., Jin, Y., 2017. A novel analytic framework of real-time multi-vessel collision risk assessment for maritime traffic surveillance. Ocean Eng. 145, 492–501.
Zhu, X., Hu, S., Li, Z., Wu, J., Yang, X., Fu, S., Han, B., 2024. Risk performance analysis approach for convoy operations via a hybrid model of STPA and DBN: a case from ice-covered waters. Ocean Eng. 302, 117570. https://doi.org/10.1016/j.oceaneng.2024.117570.